

Hadron and lepton properties from dispersion relations

Bastian Kubis

HISKP (Theorie) & BCTP
Universität Bonn, Germany

International School of Nuclear Physics, 44th Course
From quarks and gluons to hadrons and nuclei
Erice, September 23, 2023



Outline

Part I: lepton properties

- anomalous magnetic moment of the muon
 - ▷ hadronic vacuum polarisation (HVP)
 - ▷ hadronic light-by-light scattering (HLbL)

→ A. Denig's talk

Part II: hadron properties

- pion–pion (re)scattering and all that
- some illustrative examples

Part III: application

- in-depth analysis: π^0 -pole contribution to HLbL

Summary / Outlook

Part I:

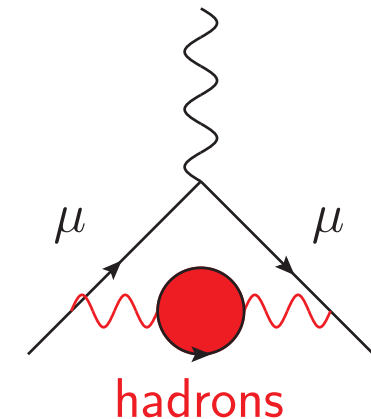
lepton properties: $(g - 2)_\mu$

Hadronic contributions to $(g - 2)_\mu$

- gyromagnetic ratio: magnetic moment \leftrightarrow spin

$$\vec{\mu} = g \frac{e}{2m} \vec{S} \quad g_\mu = 2(1 + a_\mu)$$

	$a_\mu [10^{-11}]$	$\Delta a_\mu [10^{-11}]$	
experiment	116 592 059.	22.	BNL E821 2006 + Fermilab 2021, 2023
QED	116 584 718.931	0.030	
electroweak	153.6	1.0	Aoyama et al. 2020
had. VP (LO)	6931.	40.	
had. VP (NLO)	-98.3	0.7	
had. LbL	92.	19.	
total	116 591 810.	43.	

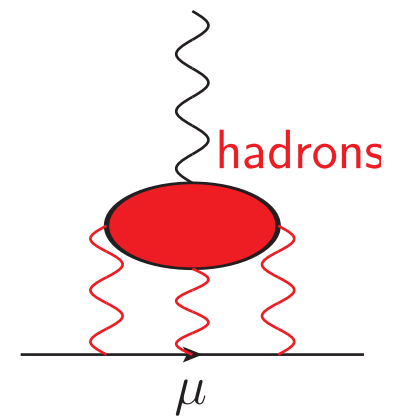


Hadronic contributions to $(g - 2)_\mu$

- gyromagnetic ratio: magnetic moment \leftrightarrow spin

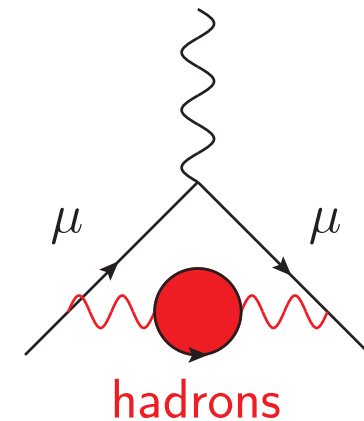
$$\vec{\mu} = g \frac{e}{2m} \vec{S} \quad g_\mu = 2(1 + a_\mu)$$

	$a_\mu [10^{-11}]$	$\Delta a_\mu [10^{-11}]$	
experiment	116 592 059.	22.	BNL E821 2006 + Fermilab 2021, 2023
QED	116 584 718.931	0.030	
electroweak	153.6	1.0	Aoyama et al. 2020
had. VP (LO)	6931.	40.	
had. VP (NLO)	-98.3	0.7	
had. LbL	92.	19.	
total	116 591 810.	43.	



Hadronic vacuum polarisation

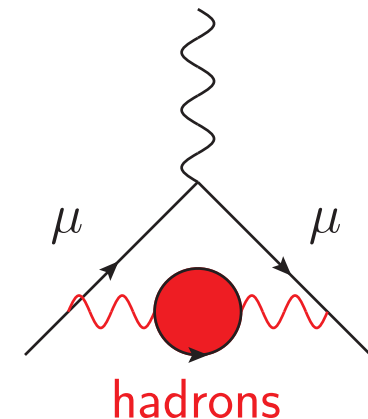
- how to control hadronic vacuum polarisation?
- characteristic **scale** set by muon mass
→ this is **not** a perturbative QCD problem!
- **dispersion relations** to the rescue:
use the optical theorem!



$$\text{Im} \quad \begin{array}{c} \gamma \\ \gamma \\ \text{hadrons} \end{array} \Leftrightarrow \left| \begin{array}{c} \gamma \\ \gamma \\ \text{hadrons} \end{array} \right|^2 \propto \sigma_{\text{tot}}(e^+e^- \rightarrow \text{hadrons})$$

Hadronic vacuum polarisation

- how to control hadronic vacuum polarisation?
- characteristic **scale** set by muon mass
→ this is **not** a perturbative QCD problem!
- **dispersion relations** to the rescue:
use the optical theorem!

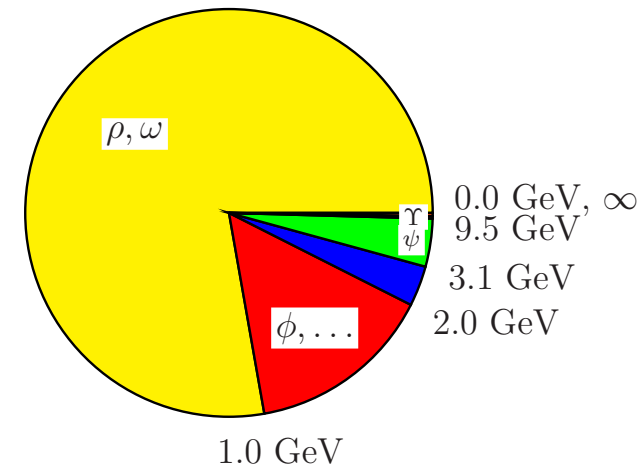


$$a_\mu^{\text{had VP}} \propto \int_{M_{\pi^0}^2}^\infty ds K(s) \sigma_{\text{tot}}(e^+ e^- \rightarrow \text{hadrons})$$

- $K(s)$: kinematical function, for large s : $K(s) \propto 1/s$,
 $\sigma_{\text{tot}}(e^+ e^- \rightarrow \text{hadrons}) \propto 1/s$
- more than 75% of $a_\mu^{\text{had VP}}$ given by energies $s \leq 1 \text{ GeV}^2$ Jegerlehner, Nyffeler 2009
- well (??) constrained by data

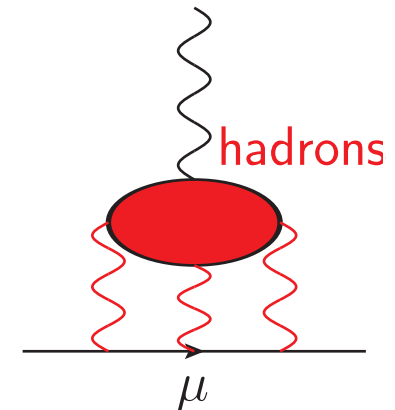
BaBar, BESIII, CMD, KLOE, SND, ...

→ *largely* an experimental task

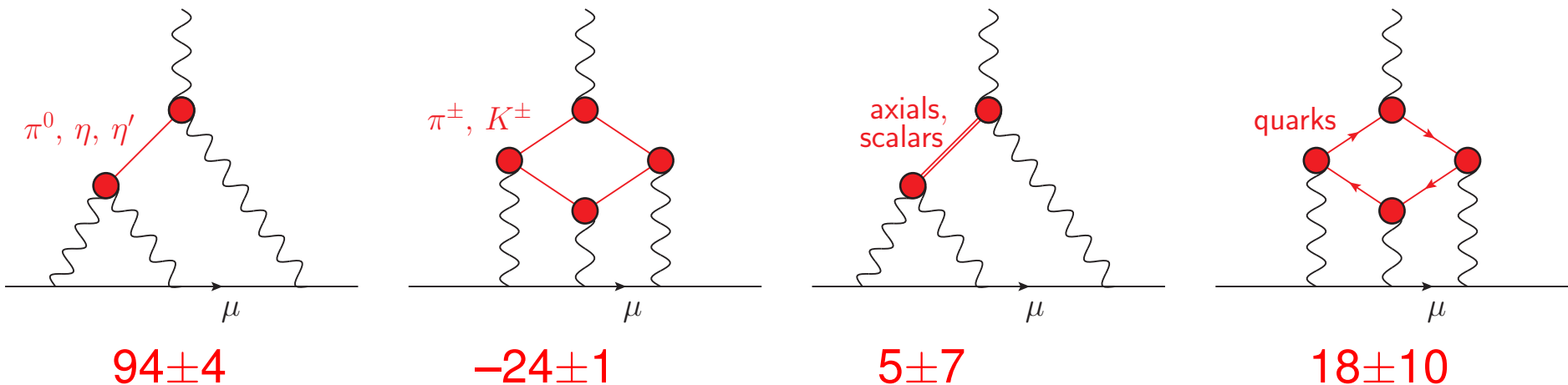


Hadronic light-by-light scattering

- hadronic light-by-light:
 - ▷ subleading in α_{QED}
 - ▷ large relative uncertainty



- different contributions calculated or estimated (in 10^{-11}):

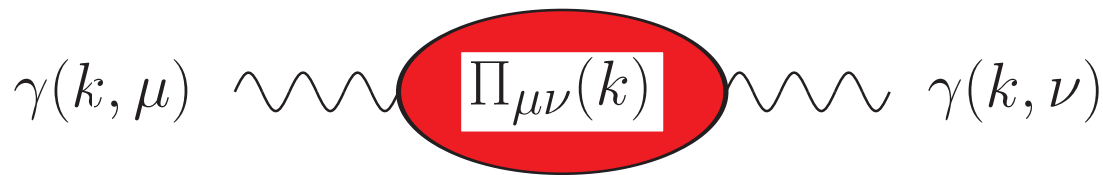


→ increasing systematic control over HLbL using
dispersion-theoretical approach

Aoyama et al. 2020

Hadronic vacuum polarisation — why so simple?

- photon two-point function:



- ▷ one single independent momentum k
- ▷ symmetric rank-2 tensor: two structures $g_{\mu\nu}, k_\mu k_\nu$
- ▷ scalar invariant can depend on one single invariant k^2
- gauge invariance: $k^\mu \Pi_{\mu\nu}(k) = 0 = k^\nu \Pi_{\mu\nu}(k)$

$$\Pi_{\mu\nu}(k) = (k^2 g_{\mu\nu} - k_\mu k_\nu) \Pi(k^2)$$

→ Lorentz + gauge invariance reduce HVP to
one single function of a single variable!

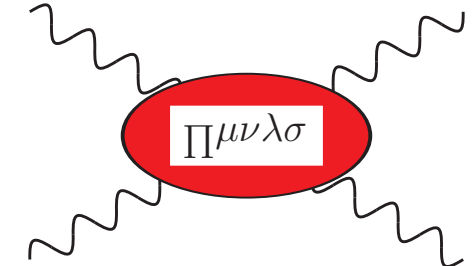
Hadronic light-by-light: dispersive approach

Colangelo, Hoferichter, Procura, Stoffer 2014, 2015

- HLbL tensor $\Pi^{\mu\nu\lambda\sigma}$: Lorentz invariance
→ 138 (136) scalar functions Eichmann et al. 2014
- gauge invariance: Bardeen, Tung 1968; Tarrach 1975

$$\Pi^{\mu\nu\lambda\sigma} = \sum_{i=1}^{54} T_i^{\mu\nu\lambda\sigma} \Pi_i$$

→ 7 distinct structures, 47 related by crossing



Hadronic light-by-light: dispersive approach

Colangelo, Hoferichter, Procura, Stoffer 2014, 2015

- HLbL tensor $\Pi^{\mu\nu\lambda\sigma}$: Lorentz invariance
→ 138 (136) scalar functions Eichmann et al. 2014
- gauge invariance: Bardeen, Tung 1968; Tarrach 1975

$$\Pi^{\mu\nu\lambda\sigma} = \sum_{i=1}^{54} T_i^{\mu\nu\lambda\sigma} \Pi_i$$

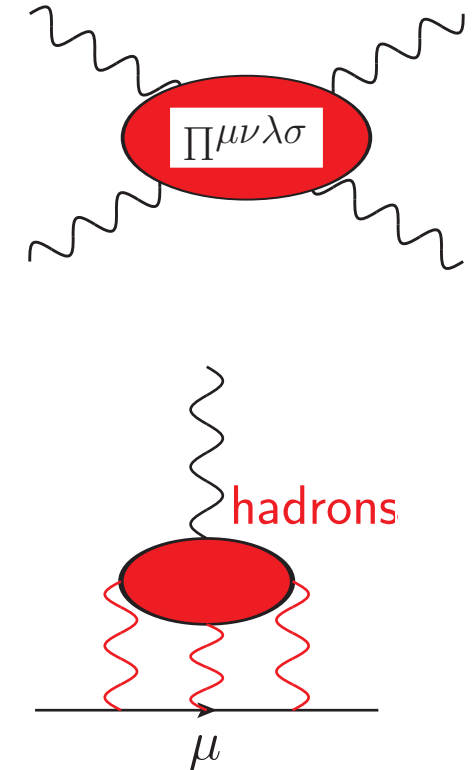
→ 7 distinct structures, 47 related by crossing

- master formula:

$$a_\mu^{\text{HLbL}} = -e^6 \int \frac{d^4 q_1}{(2\pi)^4} \frac{d^4 q_2}{(2\pi)^4} \frac{\sum_{i=1}^{12} \hat{T}_i(q_1, q_2; p) \hat{\Pi}_i(q_1, q_2, -q_1 - q_2)}{q_1^2 q_2^2 (q_1 + q_2)^2 [(p + q_1)^2 - m_\mu^2] [(p - q_2)^2 - m_\mu^2]}$$

- \hat{T}_i : known kernels

$\hat{\Pi}_i$: dispersively ↔ measurable form factors / scatt. amplitudes



Part II:

hadron properties: form factors & (re)scattering

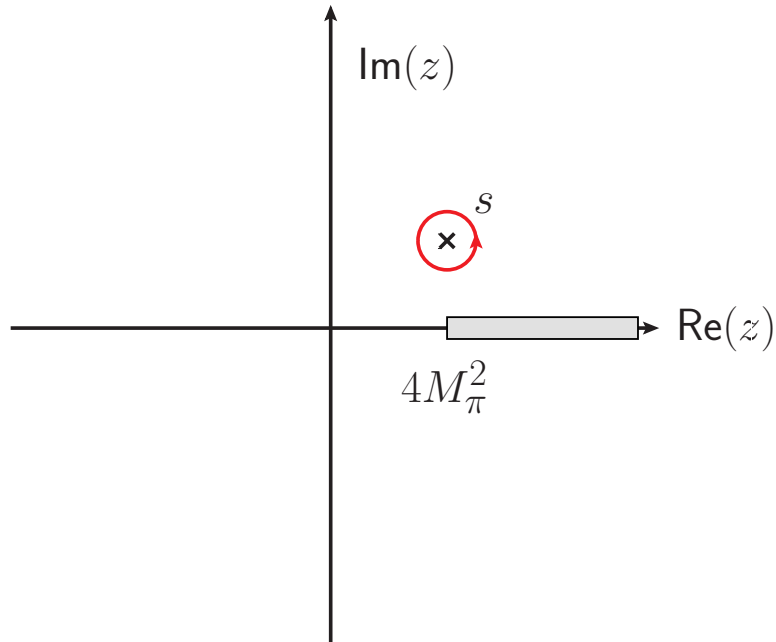
Dispersion relations for pedestrians

→ A. Pilloni's talk

analyticity (\simeq causality)

& Cauchy's theorem:

$$T(s) = \frac{1}{2\pi i} \oint_{\partial\Omega} \frac{T(z)dz}{z - s}$$

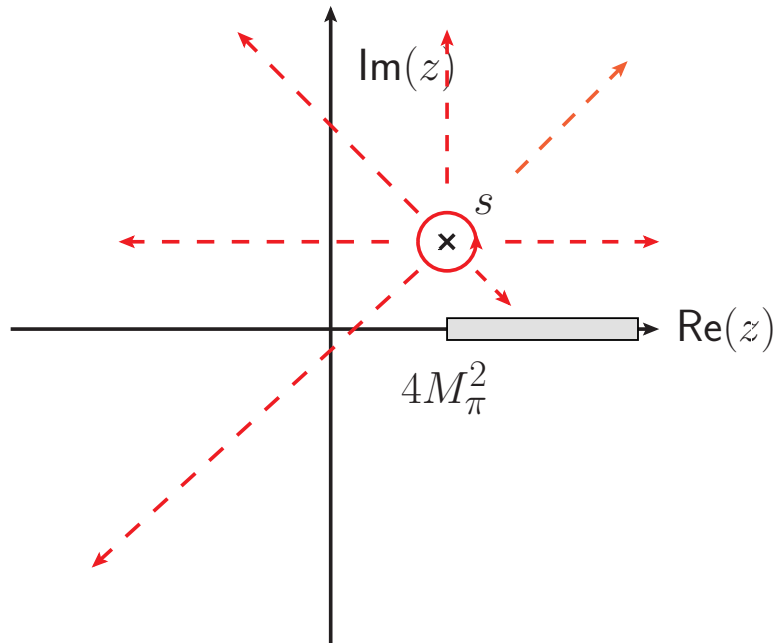


Dispersion relations for pedestrians

→ A. Pilloni's talk

analyticity (\simeq causality)

& Cauchy's theorem:

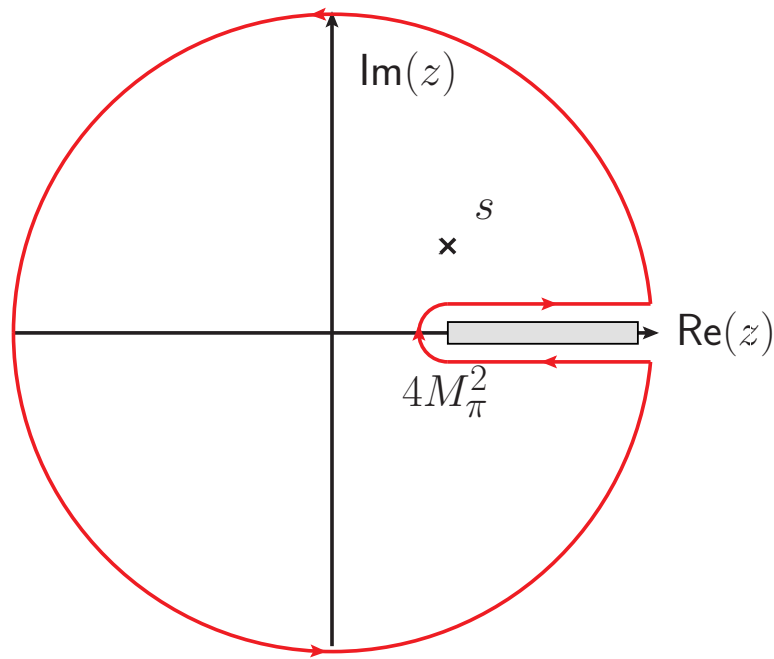


$$T(s) = \frac{1}{2\pi i} \oint_{\partial\Omega} \frac{T(z)dz}{z - s}$$

Dispersion relations for pedestrians

→ A. Pilloni's talk

analyticity (\simeq causality)
& Cauchy's theorem:

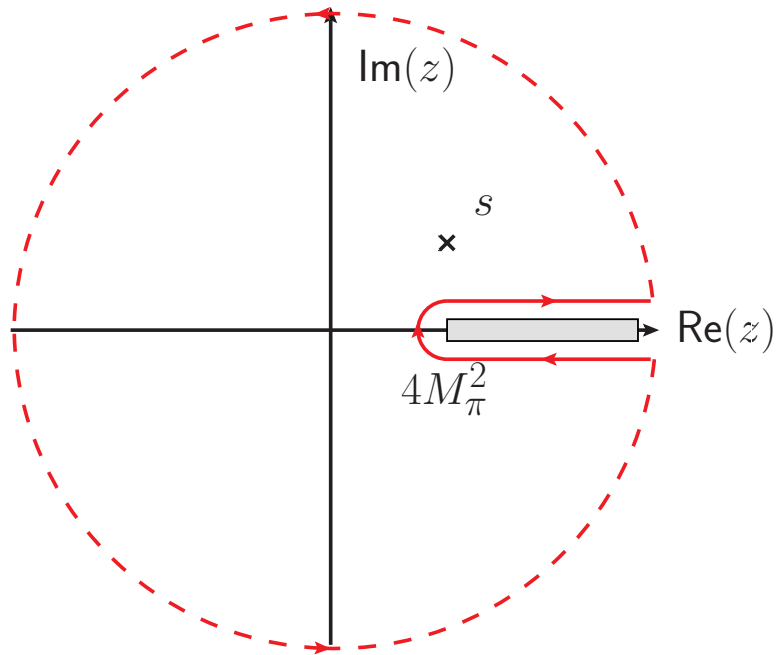


$$T(s) = \frac{1}{2\pi i} \oint_{\partial\Omega} \frac{T(z)dz}{z - s}$$

Dispersion relations for pedestrians

→ A. Pilloni's talk

analyticity (\simeq causality)
& Cauchy's theorem:



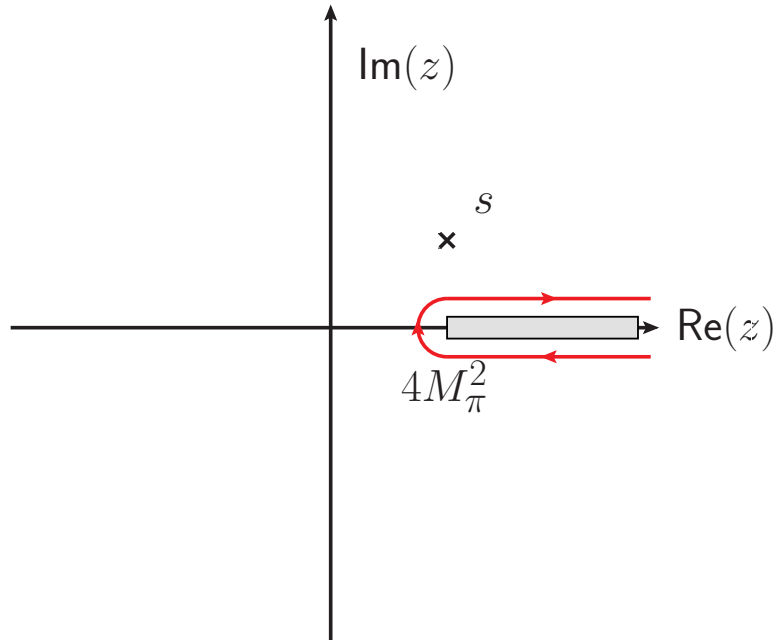
$$T(s) = \frac{1}{2\pi i} \oint_{\partial\Omega} \frac{T(z)dz}{z - s}$$

Dispersion relations for pedestrians

→ A. Pilloni's talk

analyticity (\simeq causality)

& Cauchy's theorem:



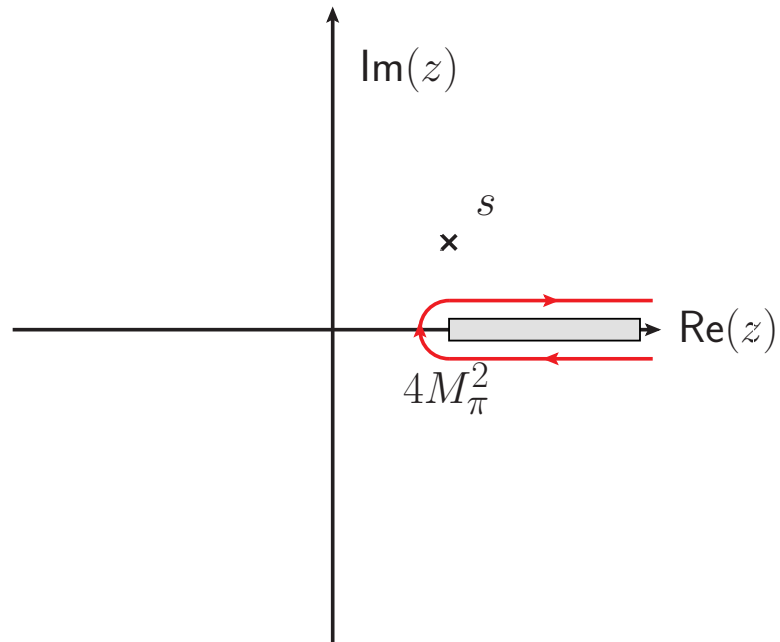
$$\begin{aligned} T(s) &= \frac{1}{2\pi i} \oint_{\partial\Omega} \frac{T(z)dz}{z-s} \\ &\rightarrow \frac{1}{2\pi i} \int_{4M_\pi^2}^\infty \frac{\text{disc } T(z)dz}{z-s} \\ &= \frac{1}{\pi} \int_{4M_\pi^2}^\infty \frac{\text{Im } T(z)dz}{z-s} \end{aligned}$$

Dispersion relations for pedestrians

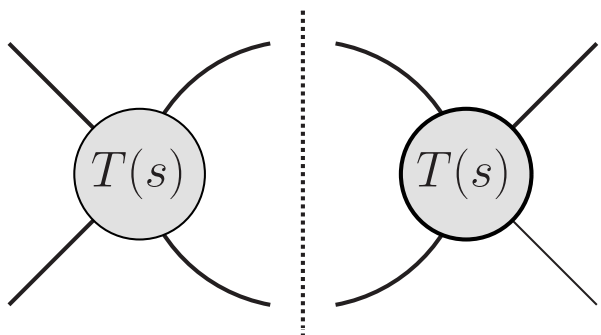
→ A. Pilloni's talk

analyticity (\simeq causality)

& Cauchy's theorem:



- $\text{disc } T(s) = 2i \text{Im } T(s)$ given by unitarity (\simeq prob. conservation):



e.g. if $T(s)$ is a $\pi\pi$ partial wave →

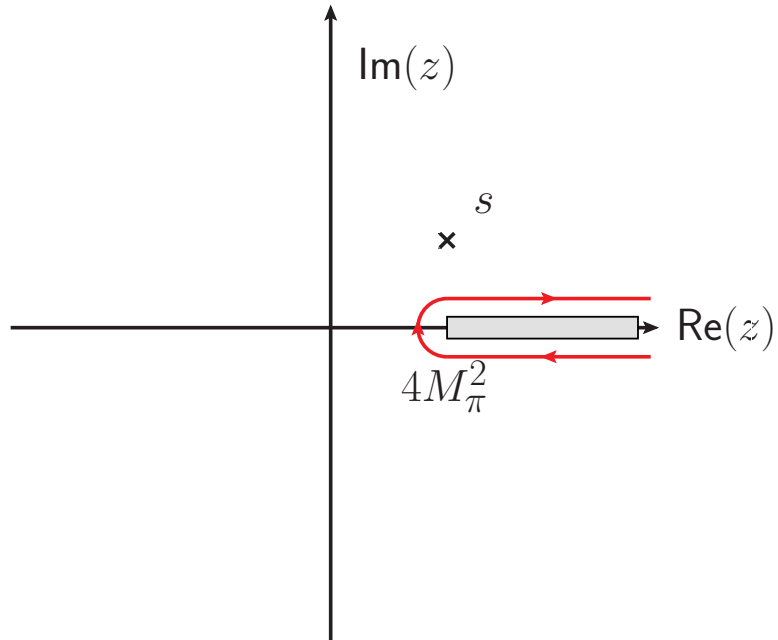
$$\frac{\text{disc } T(s)}{2i} = \text{Im } T(s) = \frac{2q_\pi}{\sqrt{s}} \theta(s - 4M_\pi^2) |T(s)|^2$$

Dispersion relations for pedestrians

→ A. Pilloni's talk

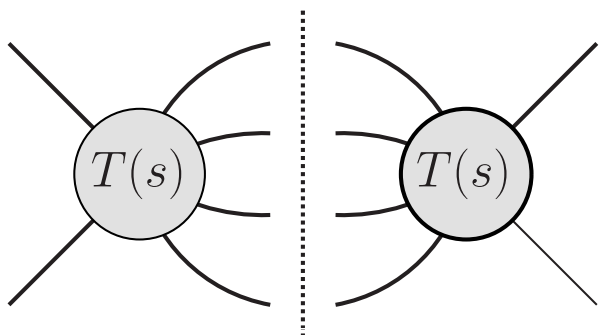
analyticity (\simeq causality)

& Cauchy's theorem:



$$\begin{aligned} T(s) &= \frac{1}{2\pi i} \oint_{\partial\Omega} \frac{T(z)dz}{z-s} \\ &\rightarrow \frac{1}{2\pi i} \int_{4M_\pi^2}^{\infty} \frac{\text{disc } T(z)dz}{z-s} \\ &= \frac{1}{\pi} \int_{4M_\pi^2}^{\infty} \frac{\text{Im } T(z)dz}{z-s} \end{aligned}$$

- $\text{disc } T(s) = 2i \text{Im } T(s)$ given by unitarity (\simeq prob. conservation):



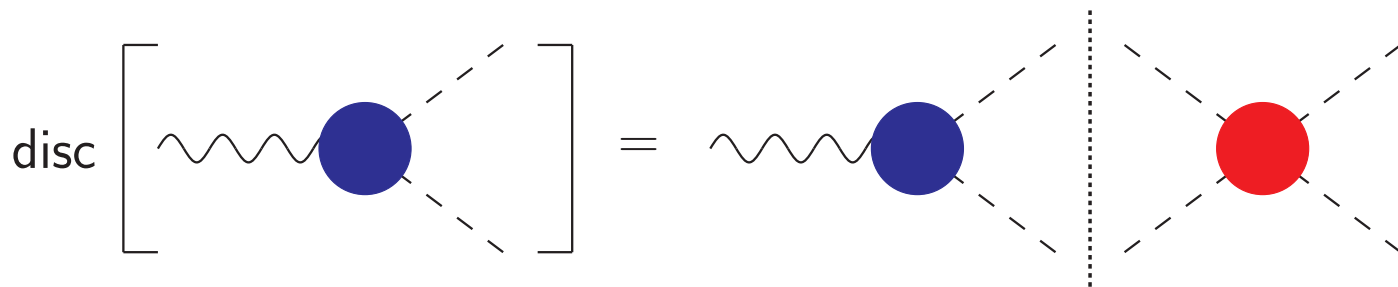
inelastic intermediate states ($K\bar{K}, 4\pi$)
suppressed at low energies
→ will often be neglected

Warm up: pion vector form factor

$$\text{disc} \left[\begin{array}{c} \text{wavy line} \\ \text{--- blue circle} \\ \text{--- dashed line} \end{array} \right] = \begin{array}{c} \text{wavy line} \\ \text{--- blue circle} \\ \text{--- dashed line} \end{array} + \begin{array}{c} \text{dotted vertical line} \\ \text{--- red circle} \\ \text{--- dashed line} \end{array}$$
$$\frac{1}{2i} \text{disc } F_\pi^V(s) = \text{Im } F_\pi^V(s) = F_\pi^V(s) \times \theta(s - 4M_\pi^2) \times \sin \delta_1^1(s) e^{-i\delta_1^1(s)}$$

→ final-state theorem: phase of $F_\pi^V(s)$ is just $\delta_1^1(s)$ Watson 1954

Warm up: pion vector form factor



$$\frac{1}{2i} \operatorname{disc} F_\pi^V(s) = \operatorname{Im} F_\pi^V(s) = F_\pi^V(s) \times \theta(s - 4 M_\pi^2) \times \sin \delta_1^1(s) e^{-i\delta_1^1(s)}$$

→ final-state theorem: phase of $F_\pi^V(s)$ is just $\delta_1^1(s)$ Watson 1954

- solution: → E. Passemar's talk; derivation → spares!

$$F_\pi^V(s) = P(s)\Omega(s) \ , \quad \Omega(s) = \exp\left\{ \frac{s}{\pi} \int_{4M_\pi^2}^\infty ds' \frac{\delta_1^1(s')}{s'(s'-s)} \right\}$$

$P(s)$ polynomial, $\Omega(s)$ Omnès function Omnès 1958

▷ $\pi\pi$ phase shifts from Roy equations

Ananthanarayan et al. 2001, García-Martín et al. 2011

▷ $P(0) = 1$ from symmetries (gauge invariance)

- below 1 GeV: $F_\pi^V(s) \approx (1 + 0.1 \text{ GeV}^{-2}s)\Omega(s)$

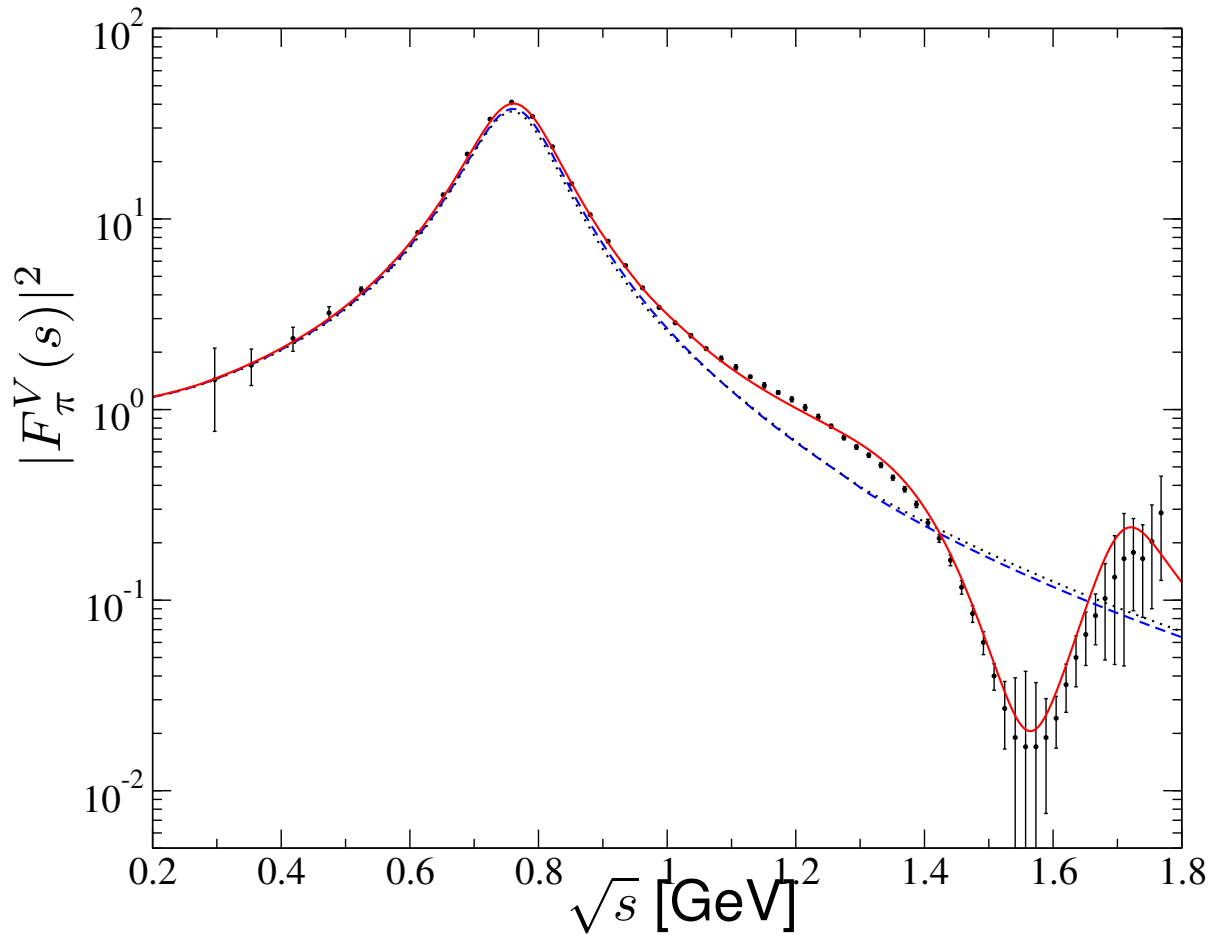
slope due to inelastic resonances $\rho', \rho'' \dots$

Hanhart 2012

Pion vector form factor vs. Omnès representation

Data on pion form factor in $\tau^- \rightarrow \pi^- \pi^0 \nu_\tau$

Belle 2008



$\pi\pi$ P-wave phase shift / effective form factor phase incl. ρ' , ρ''

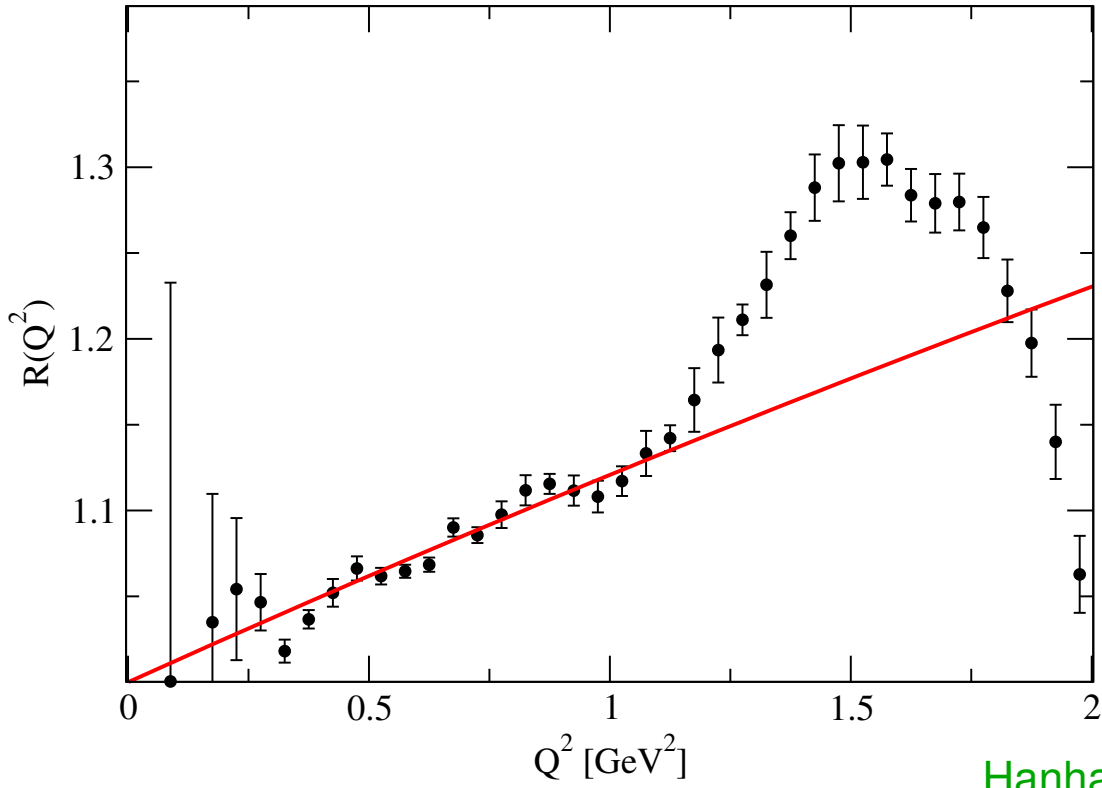
Schneider et al. 2012

Pion vector form factor vs. Omnès representation

Data on pion form factor in $\tau^- \rightarrow \pi^- \pi^0 \nu_\tau$

Belle 2008

- divide $\tau^- \rightarrow \pi^- \pi^0 \nu_\tau$ form factor by Omnès function:



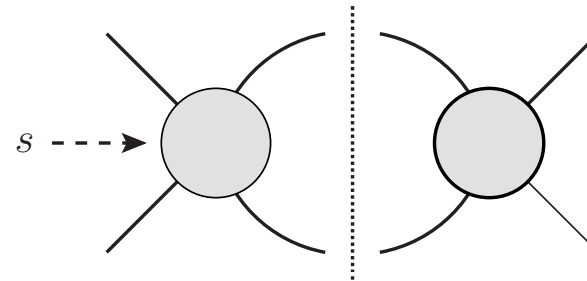
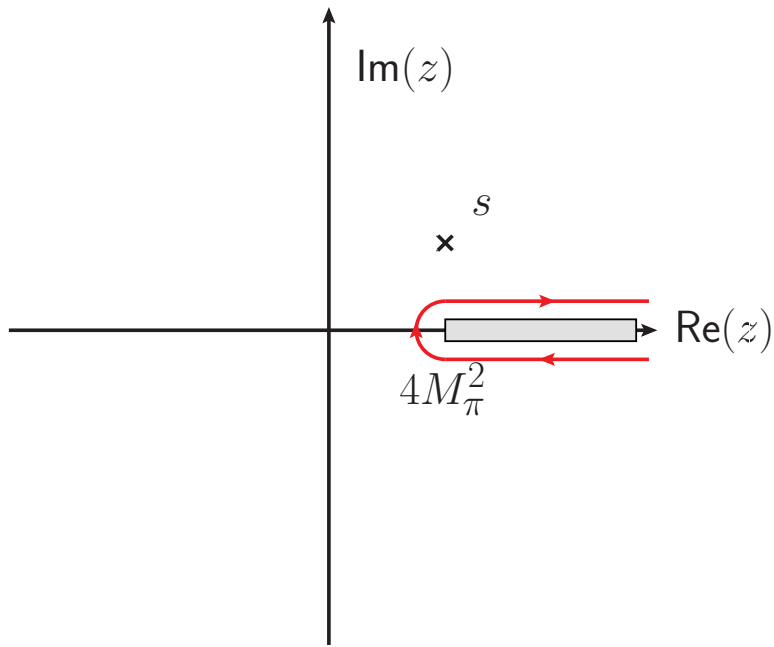
Hanhart et al. 2013

→ linear below 1 GeV: $F_\pi^V(s) \approx (1 + 0.1 \text{ GeV}^{-2}s)\Omega(s)$

→ above: inelastic resonances ρ' , ρ'' ...

What are left-hand cuts?

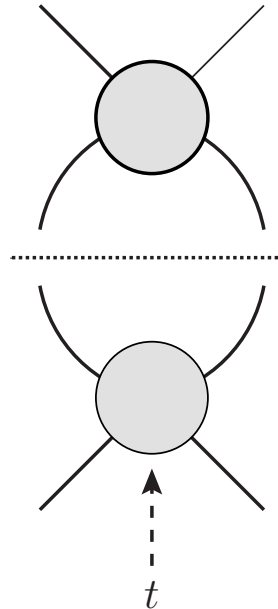
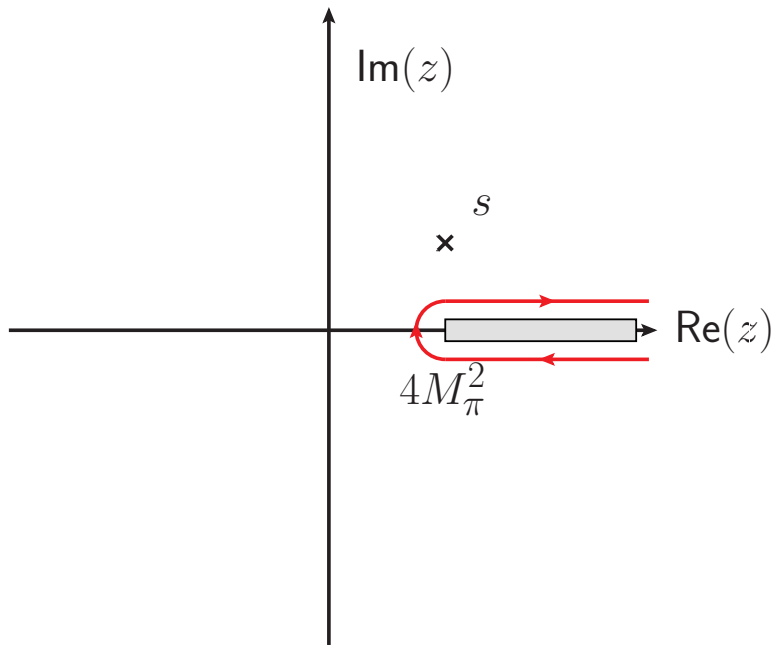
Example: pion–pion scattering



- right-hand cut due to **unitarity**: $s \geq 4M_\pi^2$

What are left-hand cuts?

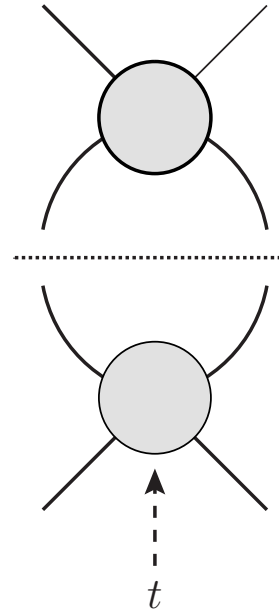
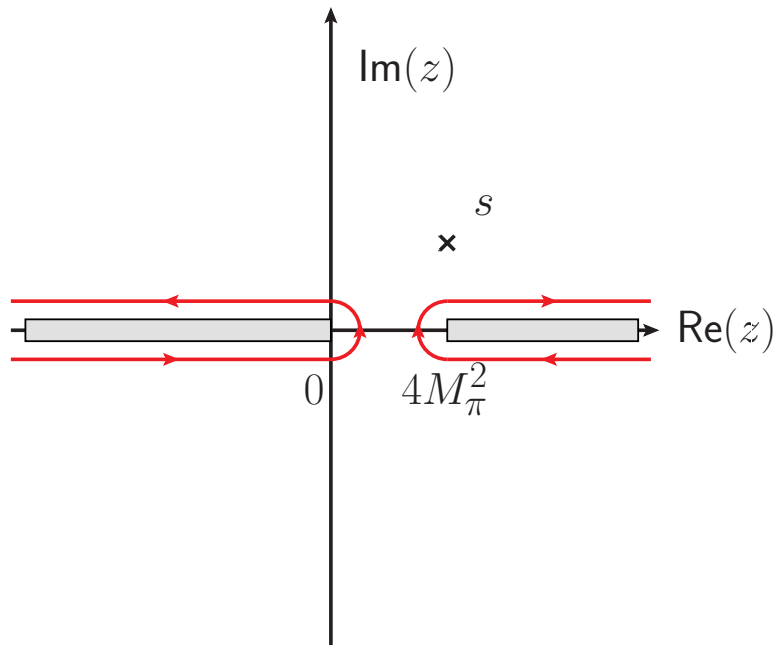
Example: pion–pion scattering



- right-hand cut due to **unitarity**: $s \geq 4M_\pi^2$
- **crossing symmetry**: cuts also for $t, u \geq 4M_\pi^2$

What are left-hand cuts?

Example: pion–pion scattering



- right-hand cut due to **unitarity**: $s \geq 4M_\pi^2$
- **crossing symmetry**: cuts also for $t, u \geq 4M_\pi^2$
- **partial-wave projection**: $T(s, t) = 32\pi \sum_i T_i(s) P_i(\cos \theta)$

$$t(s, \cos \theta) = \frac{1 - \cos \theta}{2} (4M_\pi^2 - s)$$

→ cut for $t \geq 4M_\pi^2$ becomes cut for $s \leq 0$ in partial wave

$\pi\pi$ scattering constrained by analyticity and unitarity

Roy equations = coupled system of partial-wave dispersion relations
+ crossing symmetry + unitarity

- twice-subtracted fixed- t dispersion relation:

$$T(s, t) = c(t) + \frac{1}{\pi} \int_{4M_\pi^2}^\infty ds' \left\{ \frac{s^2}{s'^2(s' - s)} + \frac{u^2}{s'^2(s' - u)} \right\} \text{Im}T(s', t)$$

- subtraction function $c(t)$ determined from crossing symmetry

$\pi\pi$ scattering constrained by analyticity and unitarity

Roy equations = coupled system of partial-wave dispersion relations
+ crossing symmetry + unitarity

- twice-subtracted fixed- t dispersion relation:

$$T(s, t) = c(t) + \frac{1}{\pi} \int_{4M_\pi^2}^\infty ds' \left\{ \frac{s^2}{s'^2(s' - s)} + \frac{u^2}{s'^2(s' - u)} \right\} \text{Im}T(s', t)$$

- subtraction function $c(t)$ determined from crossing symmetry
- project onto partial waves $t_J^I(s)$ (angular momentum J , isospin I)
→ coupled system of partial-wave integral equations

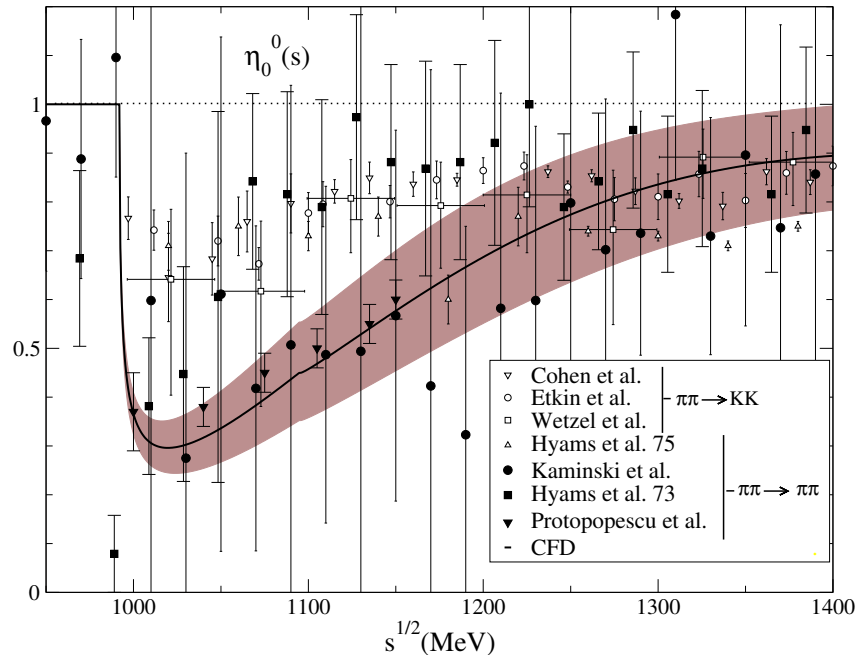
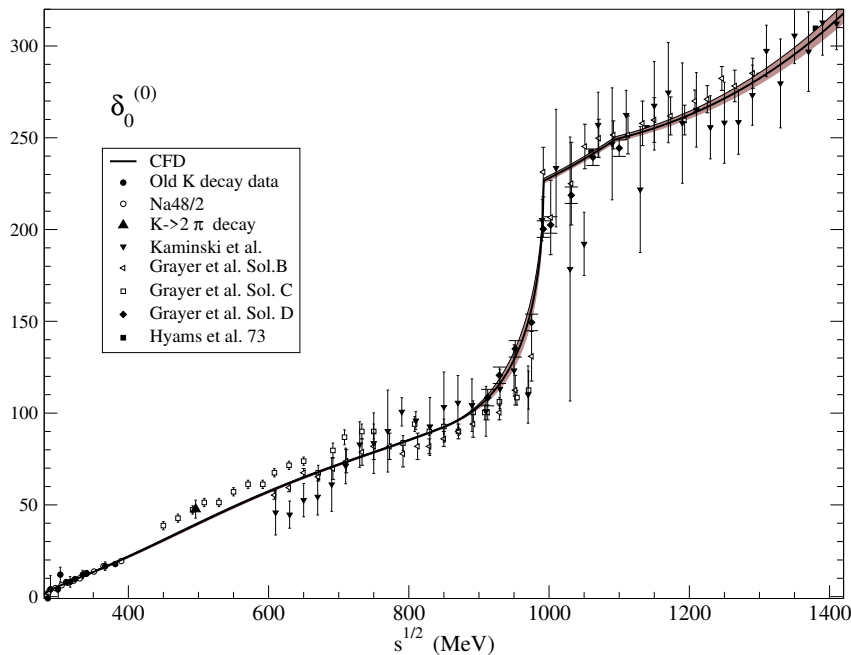
$$t_J^I(s) = k_J^I(s) + \sum_{I'=0}^2 \sum_{J'=0}^\infty \int_{4M_\pi^2}^\infty ds' K_{JJ'}^{II'}(s, s') \text{Im}t_{J'}^{I'}(s')$$

Roy 1971

- subtraction polynomial $k_J^I(s)$: $\pi\pi$ scattering lengths
can be matched to chiral perturbation theory Colangelo et al. 2001
- kernel functions $K_{JJ'}^{II'}(s, s')$ known analytically

$\pi\pi$ scattering constrained by analyticity and unitarity

- elastic unitarity \rightarrow coupled integral equations for phase shifts
- modern precision analyses:
 - $\triangleright \pi\pi$ scattering Ananthanarayan et al. 2001, García-Martín et al. 2011
 - $\triangleright \pi K$ scattering Büttiker et al. 2004, Peláez, Rodas 2020
- example: $\pi\pi I = 0$ S-wave phase shift & inelasticity

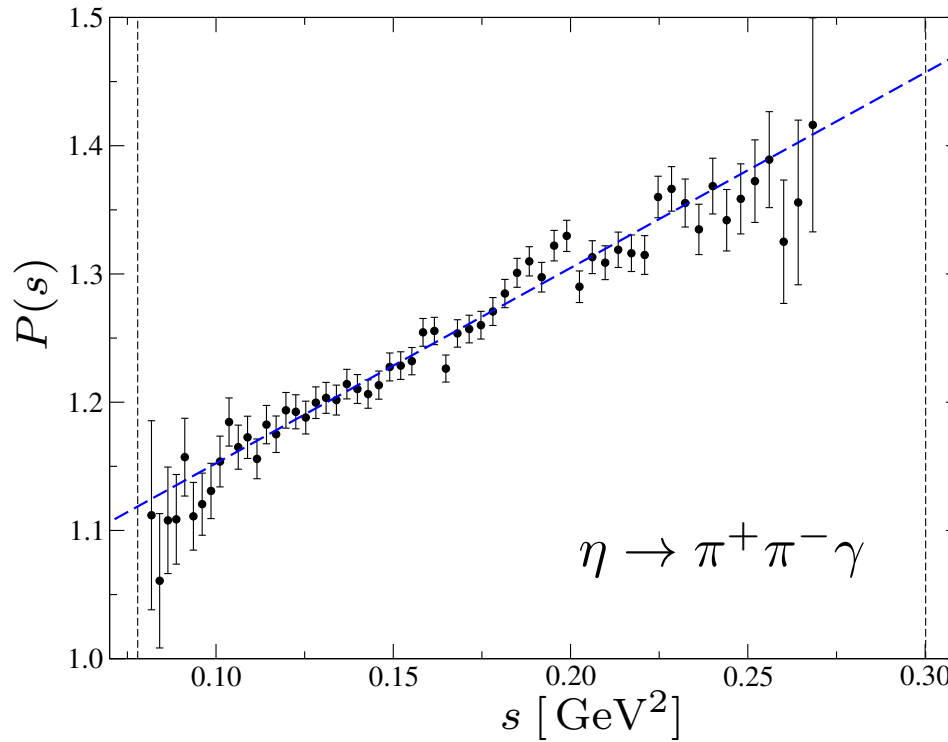


García-Martín et al. 2011

- strong constraints on data from analyticity and unitarity!

Final-state universality: $\eta, \eta' \rightarrow \pi^+ \pi^- \gamma$

- $\eta^{(\prime)} \rightarrow \pi^+ \pi^- \gamma$ driven by the chiral anomaly, $\pi^+ \pi^-$ in P-wave
→ final-state interactions the same as for vector form factor
- ansatz: $\mathcal{F}_{\pi\pi\gamma}^{\eta^{(\prime)}} = A \times P(s) \times \Omega(s)$, $P(s) = 1 + \alpha^{(\prime)} s$, $s = M_{\pi\pi}^2$
- divide data by pion form factor → $P(s)$ Stollenwerk et al. 2012

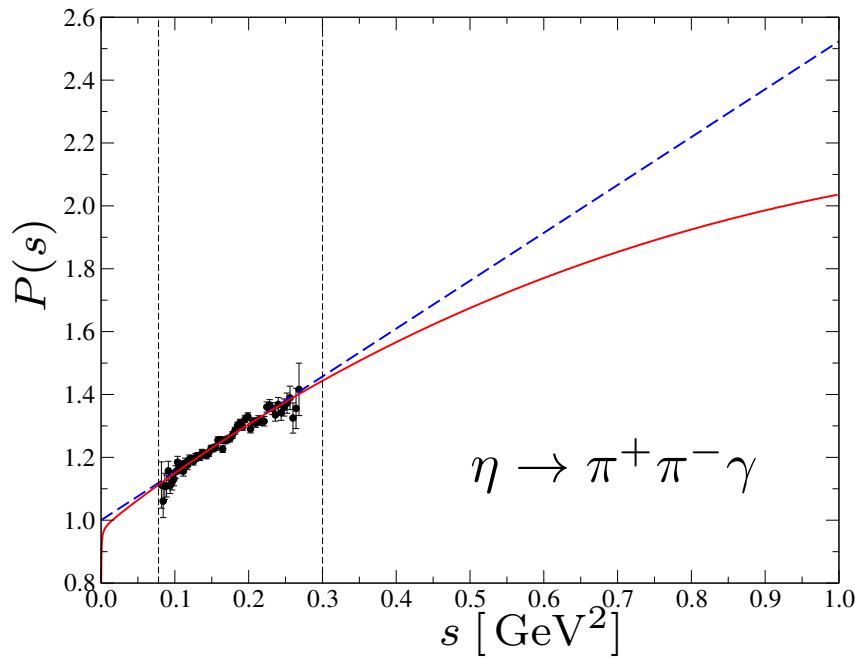
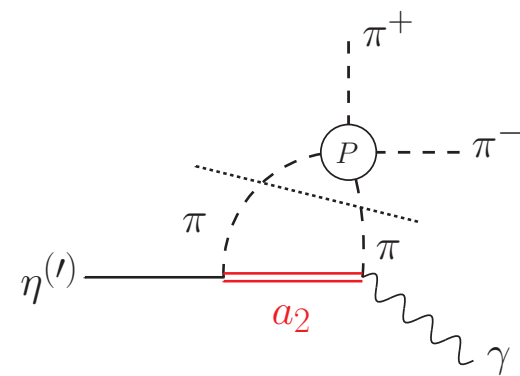
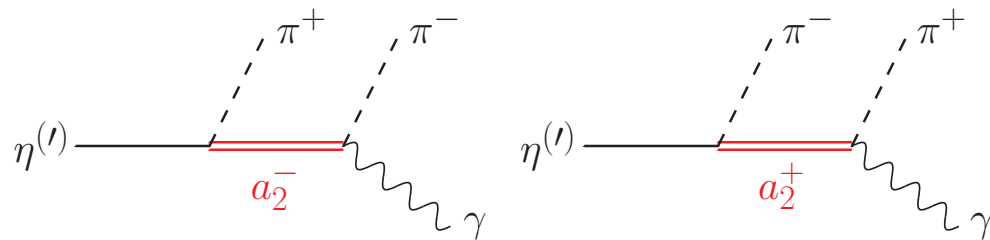


→ exp.: $\alpha_{\text{KLOE}} = (1.52 \pm 0.06) \text{ GeV}^{-2}$

cf. KLOE 2013

$\eta, \eta' \rightarrow \pi^+ \pi^- \gamma$ with left-hand cuts

- include a_2 : leading resonance in $\pi\eta^{(')}$

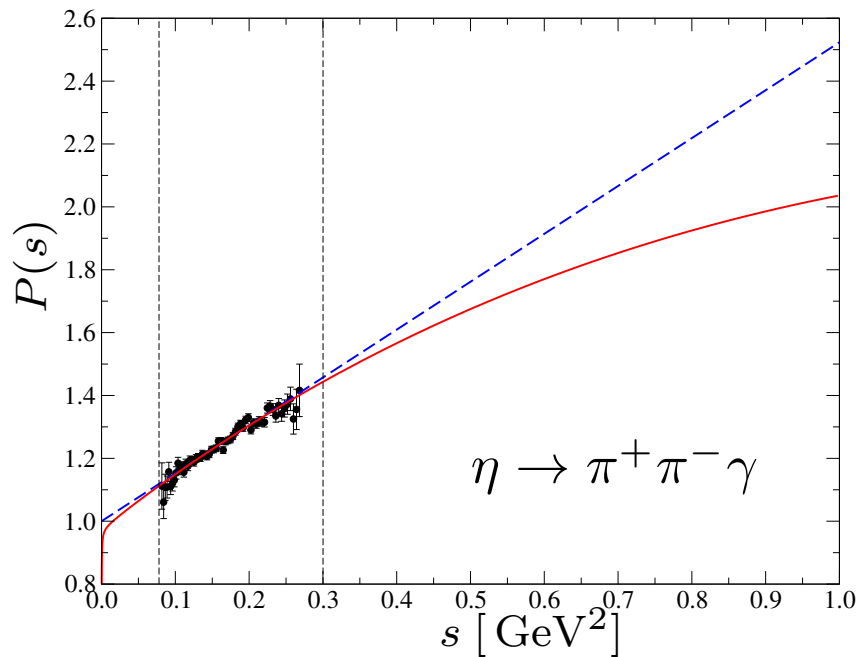
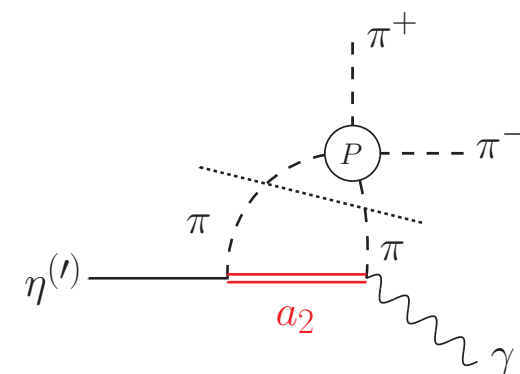
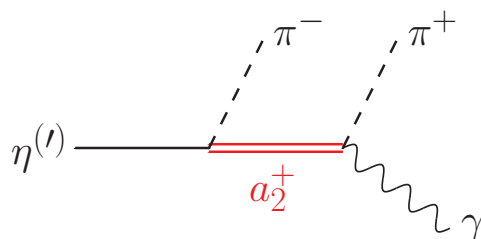
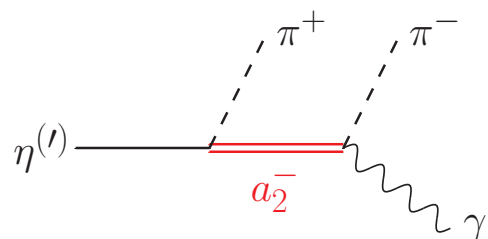


KLOE 2013; BK, Plenter 2015

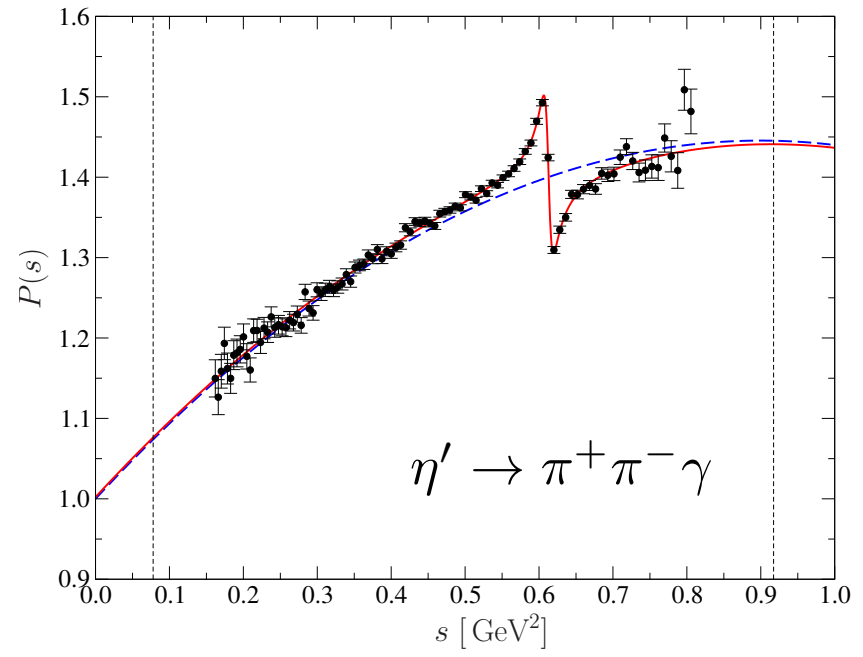
- induces **curvature** in $P(s)$

$\eta, \eta' \rightarrow \pi^+ \pi^- \gamma$ with left-hand cuts

- include a_2 : leading resonance in $\pi\eta^{(')}$



KLOE 2013; BK, Plenter 2015



BESIII 2017; Hanhart et al. 2017

- induces **curvature** in $P(s)$

- curvature, plus ρ - ω mixing

Part III:

π^0 -pole contribution

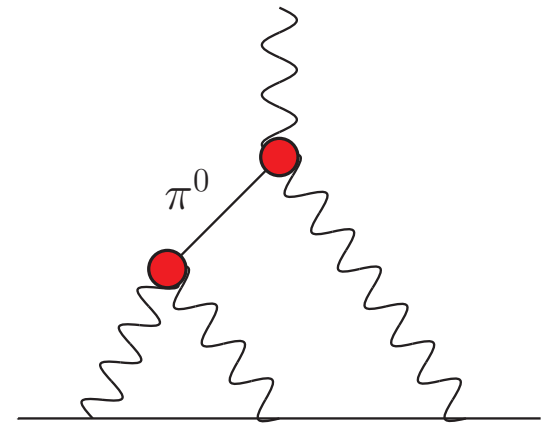
Hadronic light-by-light: the π^0 pole

- largest individual HLbL contribution:

π^0 -pole term

singly / doubly virtual transition
form factors (TFFs)

$F_{\pi^0\gamma^*\gamma^*}(q^2, 0)$ and $F_{\pi^0\gamma^*\gamma^*}(q_1^2, q_2^2)$



- normalisation fixed by Wess–Zumino–Witten (WZW) anomaly
(= full leading-order ChPT prediction):

$$F_{\pi^0\gamma^*\gamma^*}(0, 0) = \frac{1}{4\pi^2 F_\pi}$$

→ measured at 0.75% (F_π : pion decay constant)

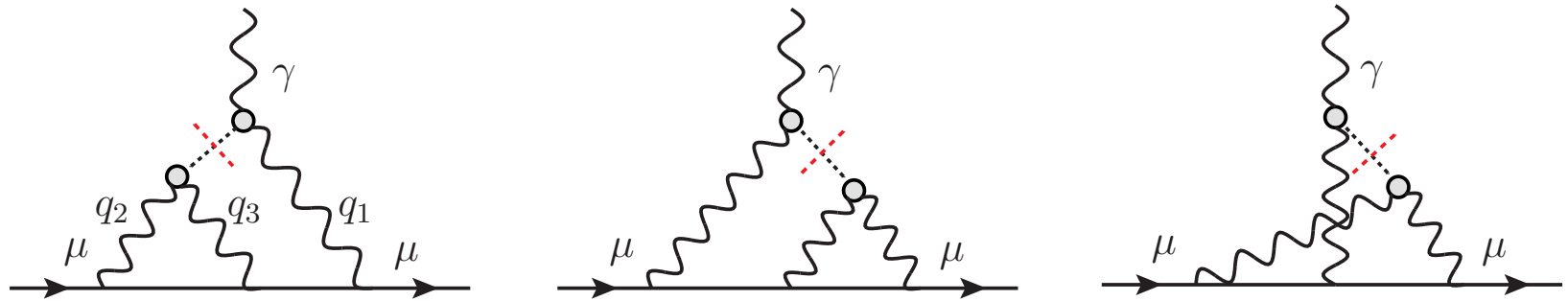
PrimEx 2020

- two-loop integral with constant form factors does not converge
 - no full prediction from e.g. chiral perturbation theory
 - sensible high-energy behaviour required!

Pion-pole contribution to a_μ

- 3-dimensional integral representation:

Jegerlehner, Nyffeler 2009



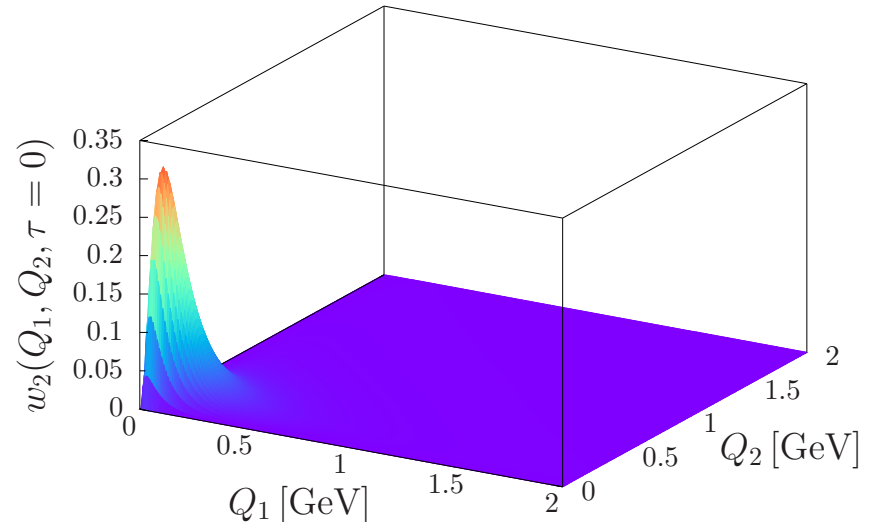
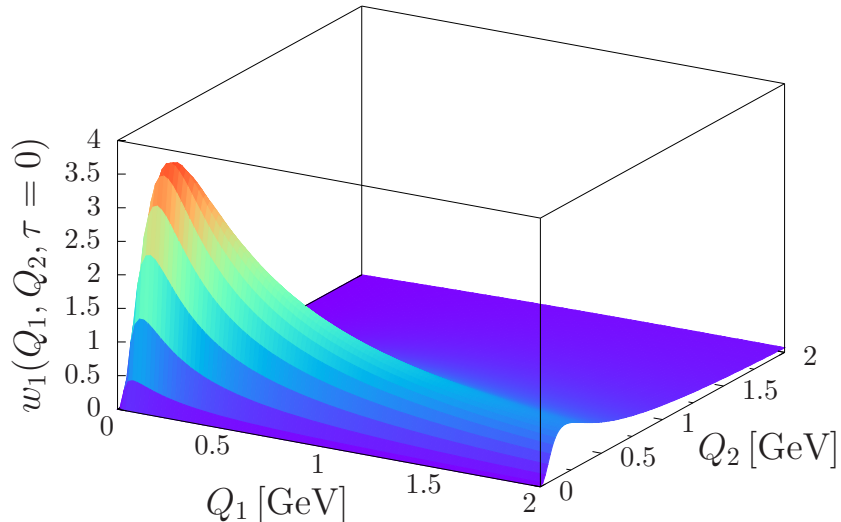
$$\begin{aligned}
 a_\mu^{\pi^0\text{-pole}} &= \left(\frac{\alpha}{\pi}\right)^3 \int_0^\infty dQ_1 \int_0^\infty dQ_2 \int_{-1}^1 d\tau \\
 &\times \left[w_1(Q_1, Q_2, \tau) F_{\pi^0\gamma^*\gamma^*}(-Q_1^2, -Q_3^2) F_{\pi^0\gamma^*\gamma^*}(-Q_2^2, 0) \right. \\
 &\quad \left. + w_2(Q_1, Q_2, \tau) F_{\pi^0\gamma^*\gamma^*}(-Q_1^2, -Q_2^2) F_{\pi^0\gamma^*\gamma^*}(-Q_3^2, 0) \right]
 \end{aligned}$$

- $w_{1/2}(Q_1, Q_2, \tau)$: kinematical weight functions, $\tau = \cos \theta$
- $F_{\pi^0\gamma^*\gamma^*}(-Q_1^2, -Q_2^2)$: space-like on-shell π^0 TFF

Pion-pole contribution to a_μ

- weight functions $w_{1/2}(Q_1, Q_2, \tau = 0)$:

Nyffeler 2016



- concentrated for $Q_i \leq 0.5 \text{ GeV}$
 - pion-pole contribution dominantly from **low-energy** region
 - pion transition form factor can be determined
model-independently and **with high precision**
using **dispersion relations**

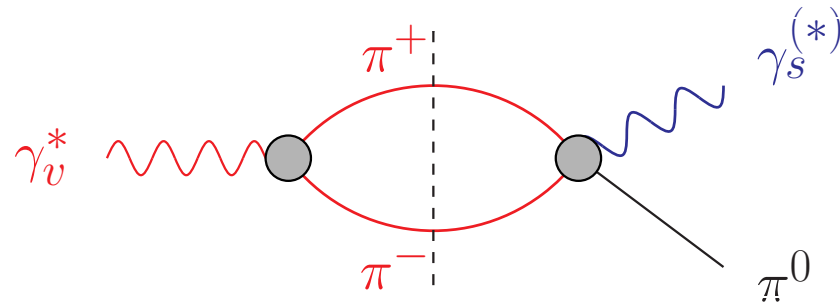
Dispersive analysis of $\pi^0 \rightarrow \gamma^*\gamma^*$

- isospin decomposition:

$$F_{\pi^0\gamma^*\gamma^*}(q_1^2, q_2^2) = F_{vs}(q_1^2, q_2^2) + F_{vs}(q_2^2, q_1^2)$$

- analyse the leading hadronic intermediate states:

Hoferichter et al. 2014



▷ isovector photon: 2 pions

\propto pion vector form factor

well known from $e^+e^- \rightarrow \pi^+\pi^-$

\times $\gamma^* \rightarrow 3\pi$ P-wave amplitude

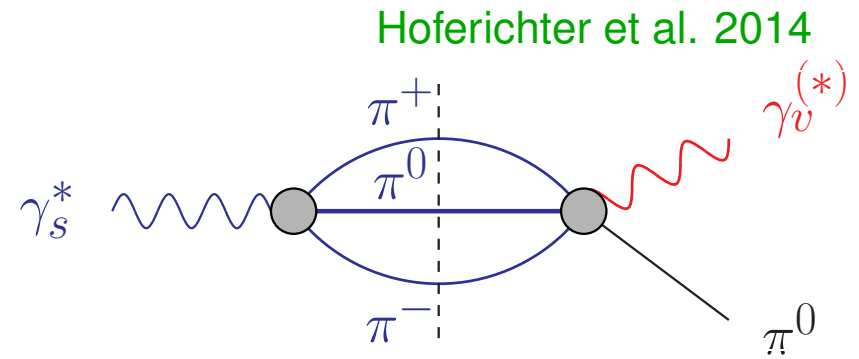
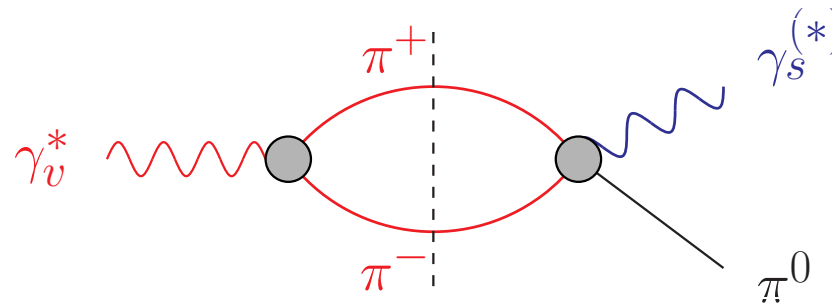
Khuri–Treiman formalism

Dispersive analysis of $\pi^0 \rightarrow \gamma^*\gamma^*$

- isospin decomposition:

$$F_{\pi^0\gamma^*\gamma^*}(q_1^2, q_2^2) = F_{vs}(q_1^2, q_2^2) + F_{vs}(q_2^2, q_1^2)$$

- analyse the leading hadronic intermediate states:



▷ isovector photon: 2 pions

\propto pion vector form factor

\times $\gamma^* \rightarrow 3\pi$ P-wave amplitude

well known from $e^+e^- \rightarrow \pi^+\pi^-$

Khuri–Treiman formalism

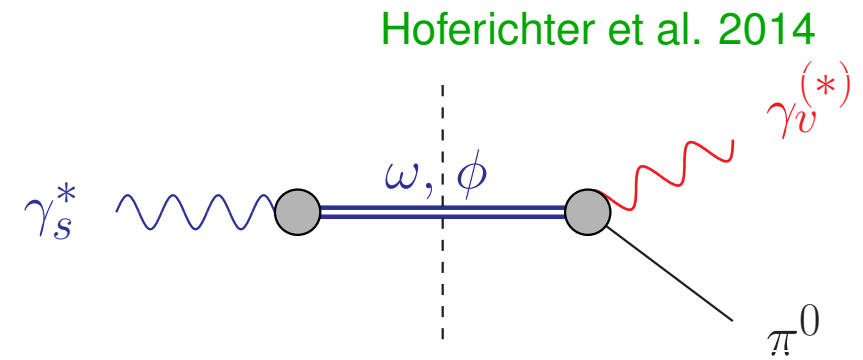
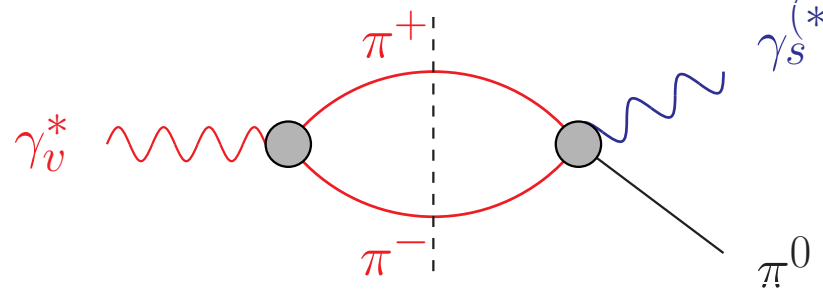
▷ isoscalar photon: 3 pions

Dispersive analysis of $\pi^0 \rightarrow \gamma^*\gamma^*$

- isospin decomposition:

$$F_{\pi^0\gamma^*\gamma^*}(q_1^2, q_2^2) = F_{vs}(q_1^2, q_2^2) + F_{vs}(q_2^2, q_1^2)$$

- analyse the leading hadronic intermediate states:



▷ isovector photon: 2 pions

\propto pion vector form factor

well known from $e^+e^- \rightarrow \pi^+\pi^-$

\times $\gamma^* \rightarrow 3\pi$ P-wave amplitude

Khuri–Treiman formalism

▷ isoscalar photon: 3 pions

dominated by narrow resonances ω, ϕ

Khuri–Treiman representation $\gamma^* \rightarrow 3\pi$

- $\gamma^*(q) \rightarrow \pi^+(p_+) \pi^-(p_-) \pi^0(p_0)$ amplitude:

$$\langle 0 | j_\mu(0) | \pi^+(p_+) \pi^-(p_-) \pi^0(p_0) \rangle = -\epsilon_{\mu\nu\rho\sigma} p_+^\nu p_-^\rho p_0^\sigma \mathcal{F}(s, t, u; q^2)$$

s, t, u : pion–pion invariant masses, $s + t + u = q^2 + 3M_\pi^2$

- “reconstruction theorem”: neglect discontinuities in F-waves...
→ decomposition into crossing-symmetric **isobars**

$$\mathcal{F}(s, t, u; q^2) = \mathcal{F}(s, q^2) + \mathcal{F}(t, q^2) + \mathcal{F}(u, q^2)$$

- normalisation fixed from Wess–Zumino–Witten anomaly:

$$\mathcal{F}(0, 0, 0; 0) = \textcolor{red}{F}_{3\pi} = \frac{1}{4\pi^2 F_\pi^3}$$

- (s -channel) P-wave projection: $f_1(s, q^2) = \mathcal{F}(s, q^2) + \hat{\mathcal{F}}(s, q^2)$
 $\hat{\mathcal{F}}(s, q^2)$: contribution from crossed channels $\mathcal{F}(t/u, q^2)$

Khuri–Treiman representation $\gamma^* \rightarrow 3\pi$

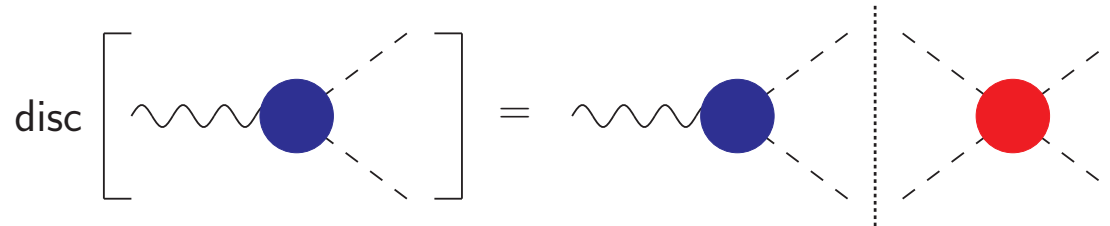
Unitarity relation for $\mathcal{F}(s, q^2 = \text{fixed})$:

$$\text{disc } \mathcal{F}(s, q^2) = 2i \left\{ \underbrace{\mathcal{F}(s, q^2)}_{\text{right-hand cut}} + \underbrace{\hat{\mathcal{F}}(s, q^2)}_{\text{left-hand cut}} \right\} \times \theta(s - 4M_\pi^2) \times \sin \delta_1^1(s) e^{-i\delta_1^1(s)}$$

Khuri–Treiman representation $\gamma^* \rightarrow 3\pi$

Unitarity relation for $\mathcal{F}(s, q^2 = \text{fixed})$:

$$\text{disc } \mathcal{F}(s, q^2) = 2i \left\{ \underbrace{\mathcal{F}(s, q^2)}_{\text{right-hand cut}} \right\} \times \theta(s - 4M_\pi^2) \times \sin \delta_1^1(s) e^{-i\delta_1^1(s)}$$



- right-hand cut only \longrightarrow Omnès problem

$$\mathcal{F}(s, q^2) = \Omega(s) a(q^2), \quad \Omega(s) = \exp \left\{ \frac{s}{\pi} \int_{4M_\pi^2}^{\infty} \frac{ds'}{s'} \frac{\delta_1^1(s')}{s' - s} \right\}$$

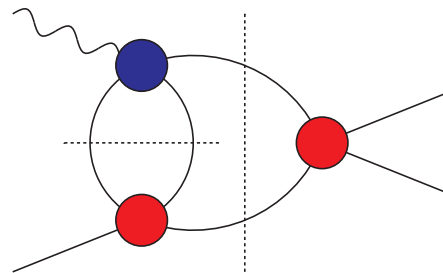
\longrightarrow amplitude given in terms of pion vector form factor

$$\mathcal{F}(s, t, u; q^2) = \text{wavy line} \text{---} \text{blue circle} \begin{matrix} \pi^+ \pi^- \\ \pi^0 \end{matrix} + \text{wavy line} \text{---} \text{blue circle} \begin{matrix} \pi^+ \\ \pi^- \pi^0 \end{matrix} + \text{wavy line} \text{---} \text{blue circle} \begin{matrix} \pi^- \\ \pi^+ \pi^0 \end{matrix}$$

Khuri–Treiman representation $\gamma^* \rightarrow 3\pi$

Unitarity relation for $\mathcal{F}(s, q^2 = \text{fixed})$:

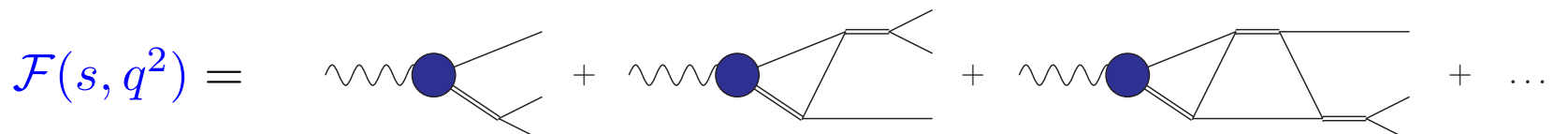
$$\text{disc } \mathcal{F}(s, q^2) = 2i \left\{ \underbrace{\mathcal{F}(s, q^2)}_{\text{right-hand cut}} + \underbrace{\hat{\mathcal{F}}(s, q^2)}_{\text{left-hand cut}} \right\} \times \theta(s - 4M_\pi^2) \times \sin \delta_1^1(s) e^{-i\delta_1^1(s)}$$



- inhomogeneities $\hat{\mathcal{F}}(s, q^2)$: angular averages over the $\mathcal{F}(t), \mathcal{F}(u)$

$$\mathcal{F}(s, q^2) = \Omega(s) \left\{ a(q^2) + \frac{s^2}{\pi} \int_{4M_\pi^2}^\infty \frac{ds'}{(s')^2} \frac{\sin \delta_1^1(s') \hat{\mathcal{F}}(s', q^2)}{|\Omega(s')|(s' - s)} \right\}$$

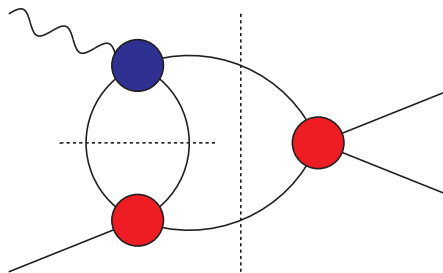
$$\hat{\mathcal{F}}(s, q^2) = \frac{3}{2} \int_{-1}^1 dz (1 - z^2) \mathcal{F}(t(s, z), q^2)$$



Khuri–Treiman representation $\gamma^* \rightarrow 3\pi$

Unitarity relation for $\mathcal{F}(s, q^2 = \text{fixed})$:

$$\text{disc } \mathcal{F}(s, q^2) = 2i \left\{ \underbrace{\mathcal{F}(s, q^2)}_{\text{right-hand cut}} + \underbrace{\hat{\mathcal{F}}(s, q^2)}_{\text{left-hand cut}} \right\} \times \theta(s - 4M_\pi^2) \times \sin \delta_1^1(s) e^{-i\delta_1^1(s)}$$



- inhomogeneities $\hat{\mathcal{F}}(s, q^2)$: angular averages over the $\mathcal{F}(t), \mathcal{F}(u)$

$$\mathcal{F}(s, q^2) = \Omega(s) \left\{ a(q^2) + \frac{s^2}{\pi} \int_{4M_\pi^2}^\infty \frac{ds'}{(s')^2} \frac{\sin \delta_1^1(s') \hat{\mathcal{F}}(s', q^2)}{|\Omega(s')|(s' - s)} \right\}$$

$$\hat{\mathcal{F}}(s, q^2) = \frac{3}{2} \int_{-1}^1 dz (1 - z^2) \mathcal{F}(t(s, z), q^2)$$

- crossed-channel scatt. between s -, t -, u -channel (left-hand cuts)

Dispersive representation $\gamma^* \rightarrow 3\pi$

- parameterisation of subtraction function $a(q^2)$

→ to be fitted to $e^+e^- \rightarrow 3\pi$ cross section data:

$$a(q^2) = \frac{F_{3\pi}}{3} + \frac{q^2}{\pi} \int_{\text{thr}}^{\infty} ds' \frac{\text{Im } \mathcal{A}(s')}{s'(s' - q^2)} + C_n(q^2)$$

- $\mathcal{A}(q^2)$ includes resonance poles:

$$\mathcal{A}(q^2) = \sum_V \frac{c_V}{M_V^2 - q^2 - i\sqrt{q^2}\Gamma_V(q^2)} \quad V = \omega, \phi, \omega', \omega''$$

c_V real

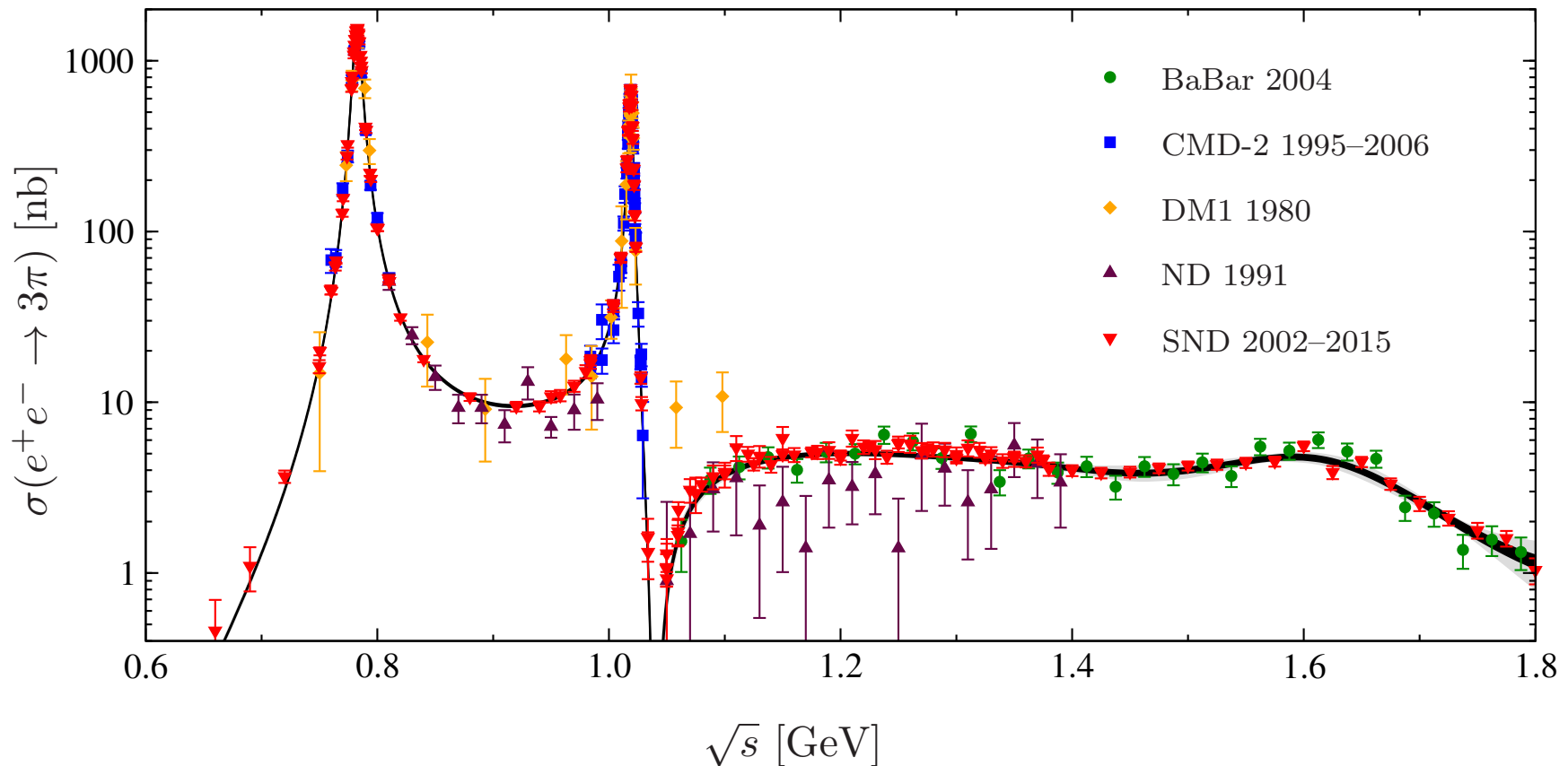
- conformal polynomial (**inelasticities**)

$$C_n(q^2) = \sum_{i=1}^n c_i \left(z(q^2)^i - z(0)^i \right), \quad z(q^2) = \frac{\sqrt{s_{\text{inel}} - s_1} - \sqrt{s_{\text{inel}} - q^2}}{\sqrt{s_{\text{inel}} - s_1} + \sqrt{s_{\text{inel}} - q^2}}$$

- **exact** implementation of $\gamma^* \rightarrow 3\pi$ anomaly:

$$\frac{F_{3\pi}}{3} = \frac{1}{\pi} \int_{s_{\text{thr}}}^{\infty} ds' \frac{\text{Im } a(s')}{s'}$$

Fit results $e^+e^- \rightarrow 3\pi$ data up to 1.8 GeV

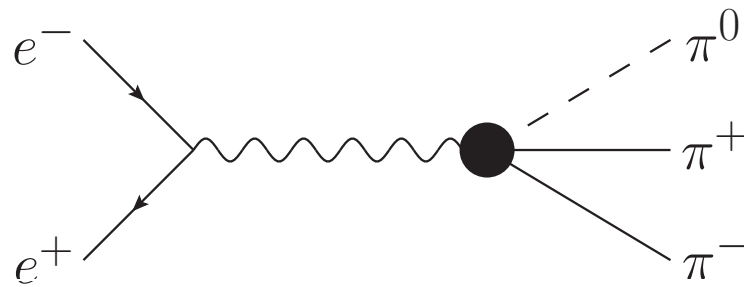


Hoferichter, Hoid, BK 2019

→ updated in Hoferichter, Hoid, BK, Schuh 2023 to include isospin breaking

- black / gray bands represent fit and total uncertainties
- vacuum polarisation removed from the cross section

From $e^+e^- \rightarrow 3\pi$ to $e^+e^- \rightarrow \pi^0\gamma^*$

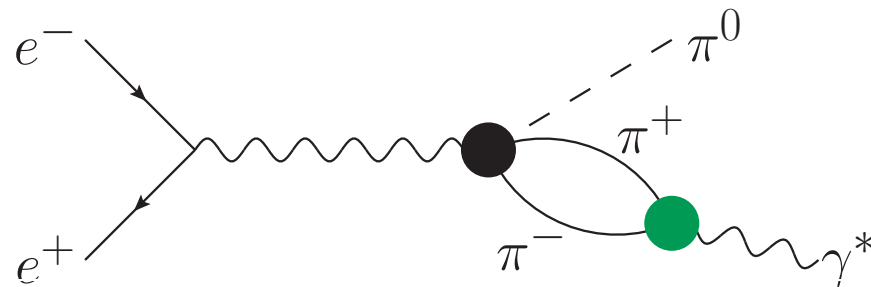


- amplitude for $e^+e^- \rightarrow 3\pi \propto \mathcal{F}(s, q^2) + \mathcal{F}(t, q^2) + \mathcal{F}(u, q^2)$

$$\mathcal{F}(s, q^2) = \Omega(s) \left\{ a(q^2) + \frac{s}{\pi} \int_{4M_\pi^2}^\infty \frac{ds'}{s'} \frac{\sin \delta_1^1(s') \hat{\mathcal{F}}(s', q^2)}{|\Omega(s')|(s' - s)} \right\}$$

subtraction function $a(q^2)$ adjusted to reproduce $e^+e^- \rightarrow 3\pi$

From $e^+e^- \rightarrow 3\pi$ to $e^+e^- \rightarrow \pi^0\gamma^*$



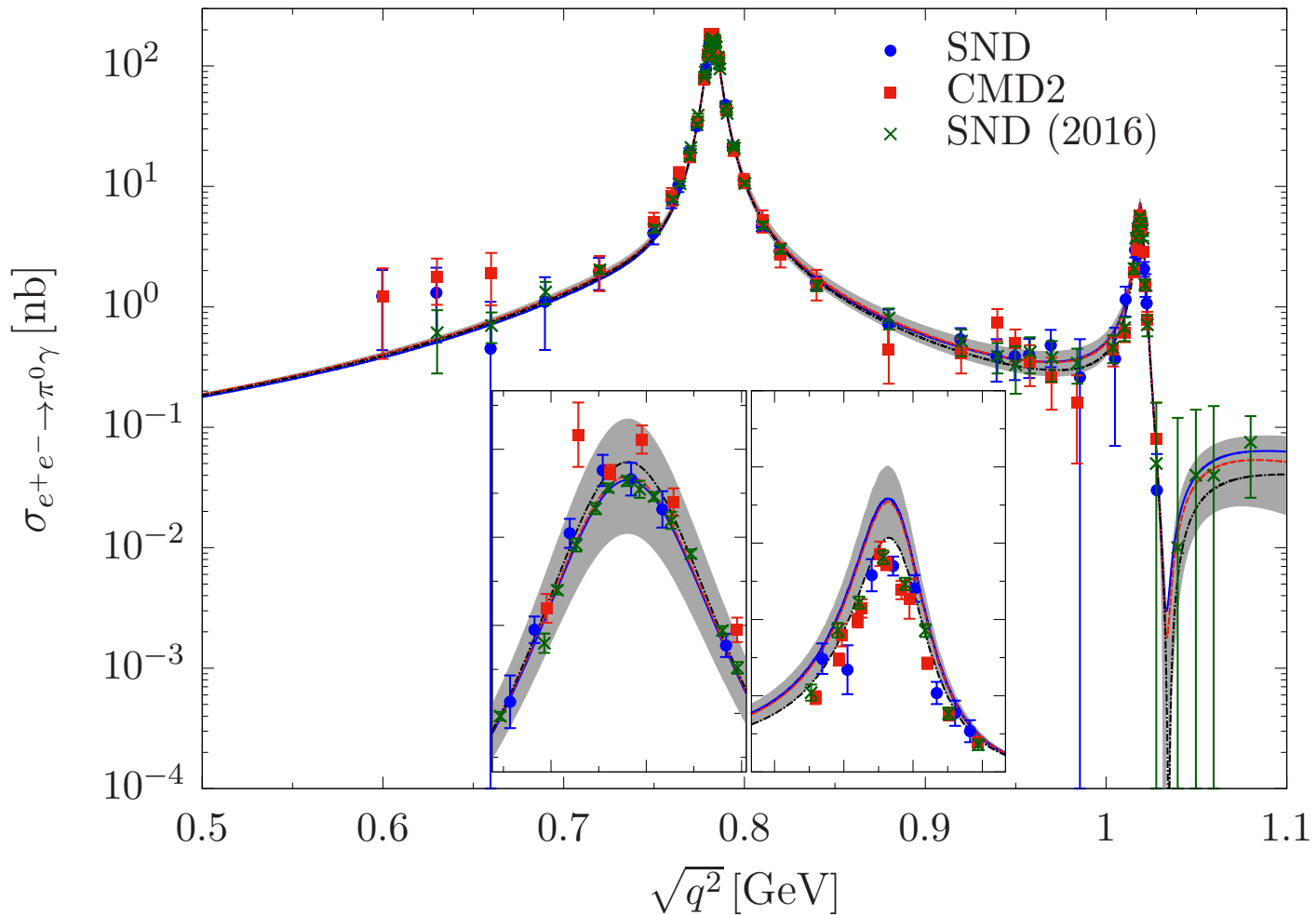
- amplitude for $e^+e^- \rightarrow 3\pi \propto \mathcal{F}(s, q^2) + \mathcal{F}(t, q^2) + \mathcal{F}(u, q^2)$

$$\mathcal{F}(s, q^2) = \Omega(s) \left\{ a(q^2) + \frac{s}{\pi} \int_{4M_\pi^2}^\infty \frac{ds'}{s'} \frac{\sin \delta_1^1(s') \hat{\mathcal{F}}(s', q^2)}{|\Omega(s')|(s' - s)} \right\}$$

subtraction function $a(q^2)$ adjusted to reproduce $e^+e^- \rightarrow 3\pi$

- fit to $e^+e^- \rightarrow 3\pi$ data
combine with $e^+e^- \rightarrow \pi^+\pi^-$ form factor
→ prediction for $e^+e^- \rightarrow \pi^0\gamma^{(*)}$

Comparison to $e^+e^- \rightarrow \pi^0\gamma$ data



Hoferichter, Hoid, BK, Leupold, Schneider 2018

- “prediction”—no further parameters adjusted
- timelike π^0 transition form factor data very well reproduced

Asymptotics and pQCD constraints (1)

- so far: dispersion relation based on (dominant) 2π , 3π
→ high precision at low energies
- double-spectral-function representation:

$$F_{\pi^0 \gamma^* \gamma^*}(q_1^2, q_2^2) = \frac{1}{\pi^2} \int_{4M_\pi^2}^\infty dx \int_{s_{\text{thr}}}^\infty dy \frac{\rho^{\text{disp}}(x, y)}{(x - q_1^2)(y - q_2^2)}$$
$$\rho^{\text{disp}}(x, y) = \frac{q_\pi^3(x)}{12\pi\sqrt{x}} \text{Im} [F_\pi^{V*}(x) f_1(x, y)] + [x \leftrightarrow y]$$

Asymptotics and pQCD constraints (1)

- so far: dispersion relation based on (dominant) 2π , 3π
→ high precision at low energies
- double-spectral-function representation:

$$F_{\pi^0\gamma^*\gamma^*}(q_1^2, q_2^2) = \frac{1}{\pi^2} \int_{4M_\pi^2}^\infty dx \int_{s_{\text{thr}}}^\infty dy \frac{\rho^{\text{disp}}(x, y)}{(x - q_1^2)(y - q_2^2)}$$

$$\rho^{\text{disp}}(x, y) = \frac{q_\pi^3(x)}{12\pi\sqrt{x}} \text{Im} [F_\pi^{V*}(x)f_1(x, y)] + [x \leftrightarrow y]$$

- asymptotically: pion wave function $\phi_\pi(x) = 6x(1-x) + \dots$

$$F_{\pi^0\gamma^*\gamma^*}(q_1^2, q_2^2) = -\frac{2F_\pi}{3} \int_0^1 dx \frac{\phi_\pi(x)}{xq_1^2 + (1-x)q_2^2} + \mathcal{O}(Q^{-4})$$

implies asymptotically

Brodsky, Lepage 1979–1981

$$F_{\pi^0\gamma^*\gamma^*}(-Q^2, -Q^2) \sim \frac{2F_\pi}{3Q^2}, \quad F_{\pi^0\gamma^*\gamma^*}(-Q^2, 0) \sim \frac{2F_\pi}{Q^2}$$

→ rewrite this as double-spectral representation $\rho^{\text{pQCD}}(x, y)$

Khodjamirian 1999; Hoferichter et al. 2018

Asymptotics and pQCD constraints (2)

- dispersion-theoretical $\rho^{\text{disp}}(x, y)$ at low energies $x, y \leq s_m$
- doubly-asymptotic $\rho^{\text{pQCD}}(x, y)$ for $x, y > s_m$
→ does not contribute to singly-virtual TFF

$$F_{\pi^0 \gamma^* \gamma^*}(q_1^2, q_2^2) = \frac{1}{\pi^2} \int_0^{s_m} dx \int_0^{s_m} dy \frac{\rho^{\text{disp}}(x, y)}{(x - q_1^2)(y - q_2^2)} + \frac{1}{\pi^2} \int_{s_m}^\infty dx \int_{s_m}^\infty dy \frac{\rho^{\text{pQCD}}(x, y)}{(x - q_1^2)(y - q_2^2)}$$

- pQCD piece alone: $F_{\pi^0 \gamma^* \gamma^*}(-Q^2, -Q^2) = \frac{2F_\pi}{3Q^2} + \mathcal{O}(Q^{-4})$

dispersive part: $\frac{1}{\pi^2} \int_0^{s_m} dx \int_0^{s_m} dy \frac{\rho^{\text{disp}}(x, y)}{(x + Q^2)(y + Q^2)} = \mathcal{O}(Q^{-4})$

Asymptotics and pQCD constraints (2)

- dispersion-theoretical $\rho^{\text{disp}}(x, y)$ at low energies $x, y \leq s_m$
- doubly-asymptotic $\rho^{\text{pQCD}}(x, y)$ for $x, y > s_m$
→ does not contribute to singly-virtual TFF

$$F_{\pi^0 \gamma^* \gamma^*}(q_1^2, q_2^2) = \frac{1}{\pi^2} \int_0^{s_m} dx \int_0^{s_m} dy \frac{\rho^{\text{disp}}(x, y)}{(x - q_1^2)(y - q_2^2)} + \frac{1}{\pi^2} \int_{s_m}^\infty dx \int_{s_m}^\infty dy \frac{\rho^{\text{pQCD}}(x, y)}{(x - q_1^2)(y - q_2^2)}$$

- pQCD piece alone: $F_{\pi^0 \gamma^* \gamma^*}(-Q^2, -Q^2) = \frac{2F_\pi}{3Q^2} + \mathcal{O}(Q^{-4})$
dispersive part: $\frac{1}{\pi^2} \int_0^{s_m} dx \int_0^{s_m} dy \frac{\rho^{\text{disp}}(x, y)}{(x + Q^2)(y + Q^2)} = \mathcal{O}(Q^{-4})$
- anomaly and Brodsky–Lepage: $\rho^{\text{disp}}(x, y)$ fulfils two sum rules
→ add effective pole: $\rho^{\text{eff}} = \frac{g_{\text{eff}}}{4\pi^2 F_\pi} \pi^2 M_{\text{eff}}^4 \delta(x - M_{\text{eff}}^2) \delta(y - M_{\text{eff}}^2)$
find $g_{\text{eff}} \sim 10\%$ (small), $M_{\text{eff}} \sim 1.5 \dots 2.0 \text{ GeV}$ (reasonable)

Uncertainties in the π^0 -pole contribution

Normalisation

- uncertainty on $\pi^0 \rightarrow \gamma\gamma$ $\pm 1.5\%$

PrimEx 2020

Dispersive input

- different $\pi\pi$ phase shift inputs:
 - ▷ Bern vs. Madrid Colangelo et al. 2011, García-Martín et al. 2011
 - ▷ effective form factor phase (incl. ρ' , ρ'') Schneider et al. 2012
- cutoff in Khuri–Treiman integrals 1.8 … 2.5 GeV

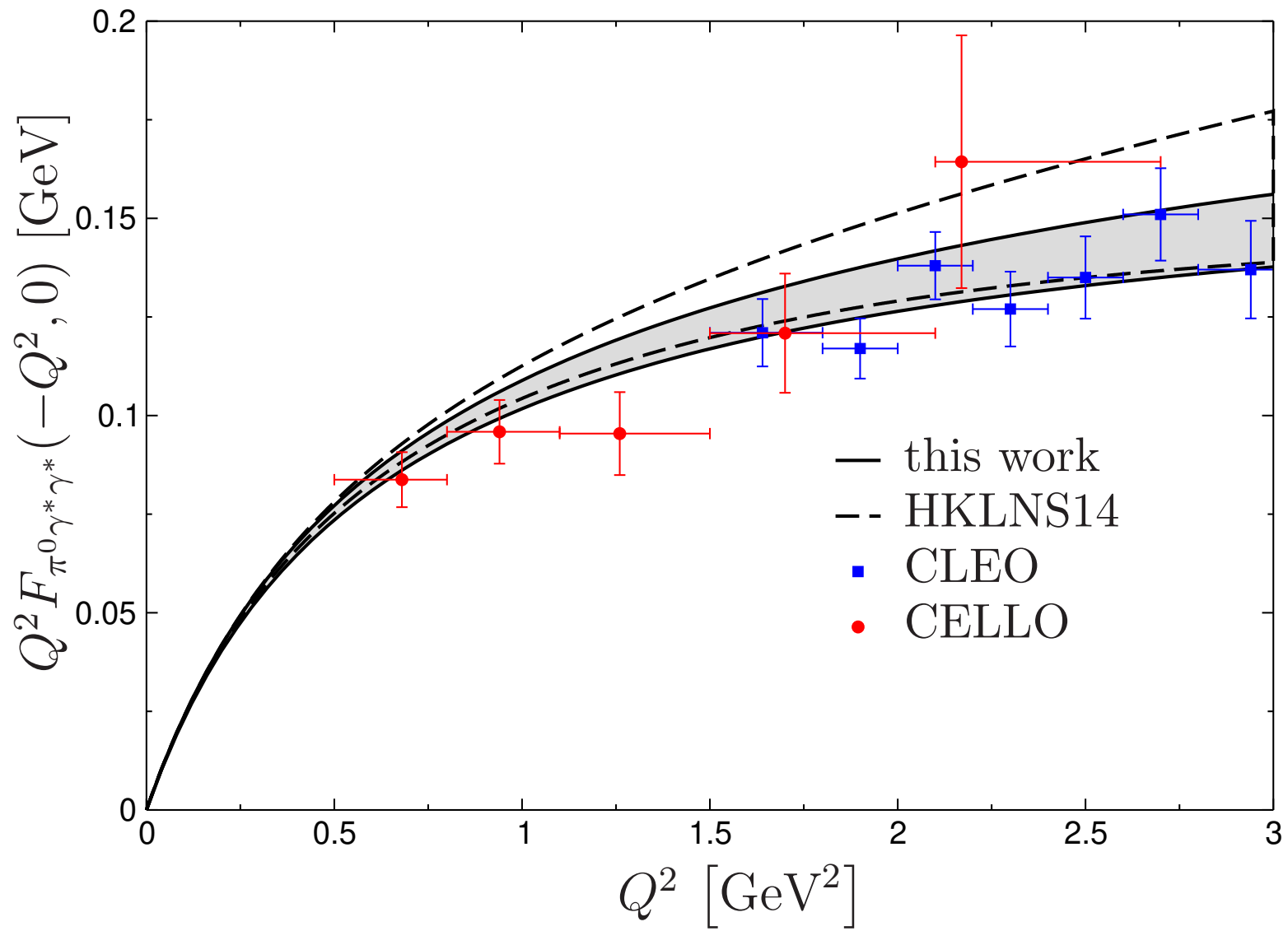
Brodsky–Lepage limit uncertainty

- allow for $\begin{array}{c} +20\% \\ -10\% \end{array}$, 3σ band around data BaBar 2009, Belle 2012

Onset of pQCD asymptotics

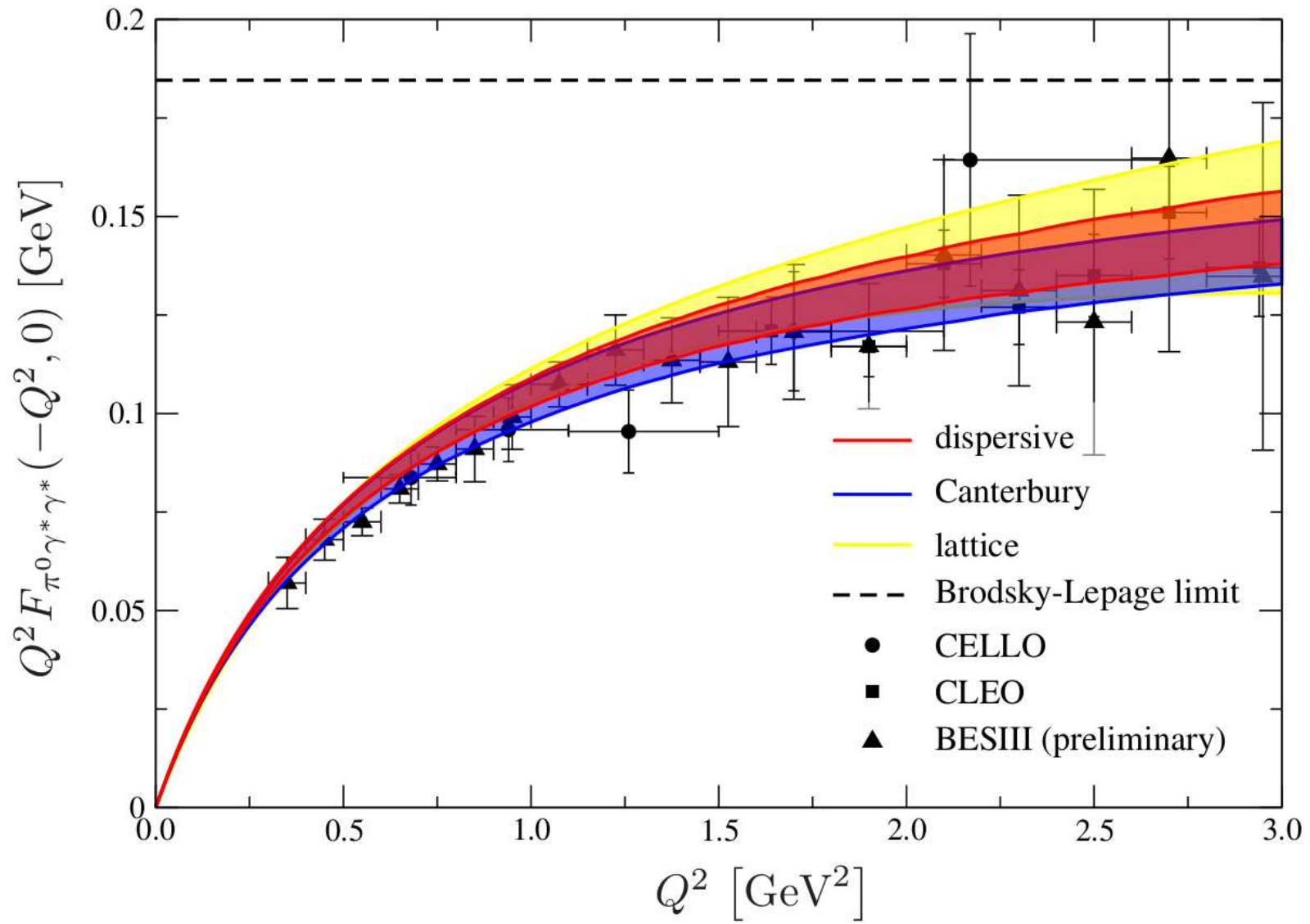
- vary $s_m = 1.7(3)\text{GeV}^2$

Results: singly-virtual



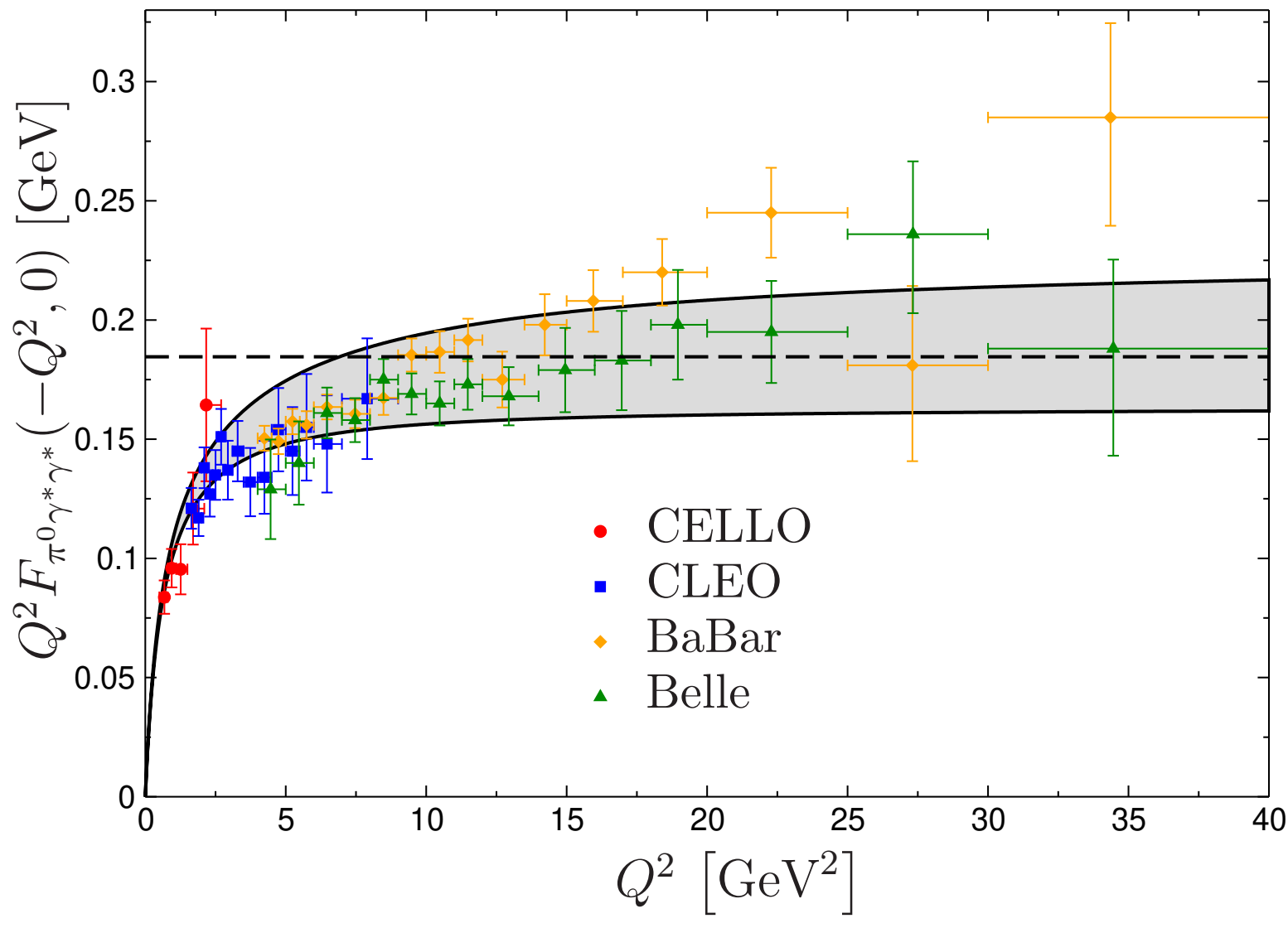
Hoferichter, Hoid, BK, Leupold, Schneider 2018

Results: singly-virtual



Aoyama et al. 2020

Results: singly-virtual



Hoferichter, Hoid, BK, Leupold, Schneider 2018

Result: $(g - 2)_\mu$ from π^0 pole

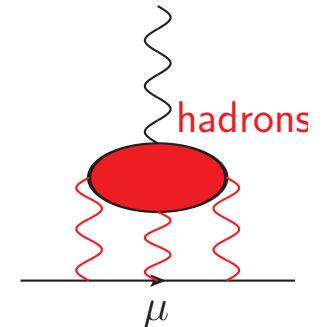
Final result for the π^0 -pole contribution [10^{-11}]

63.0 ± 0.9	chiral anomaly / $\pi^0 \rightarrow \gamma\gamma$
± 1.1	dispersive input
± 2.2 $- 1.4$	Brodsky–Lepage
± 0.6	onset of pQCD contribution s_m
$= 63.0 \pm 2.7$ $- 2.1$	Hoferichter, Hoid, BK, Leupold, Schneider 2018

- model-independent, data-driven determination
with all physical low- and high-energy constraints implemented
- perfectly consistent with
 - ▷ Padé approxim. $63.6(2.7) \times 10^{-11}$ Masjuan, Sánchez-Puertas 2017
 - ▷ lattice $62.3(2.3) \times 10^{-11}$ Gérardin et al. 2019
 - ▷ Dyson–Schw. $62.6(1.3) \times 10^{-11}$ Eichmann et al. 2019

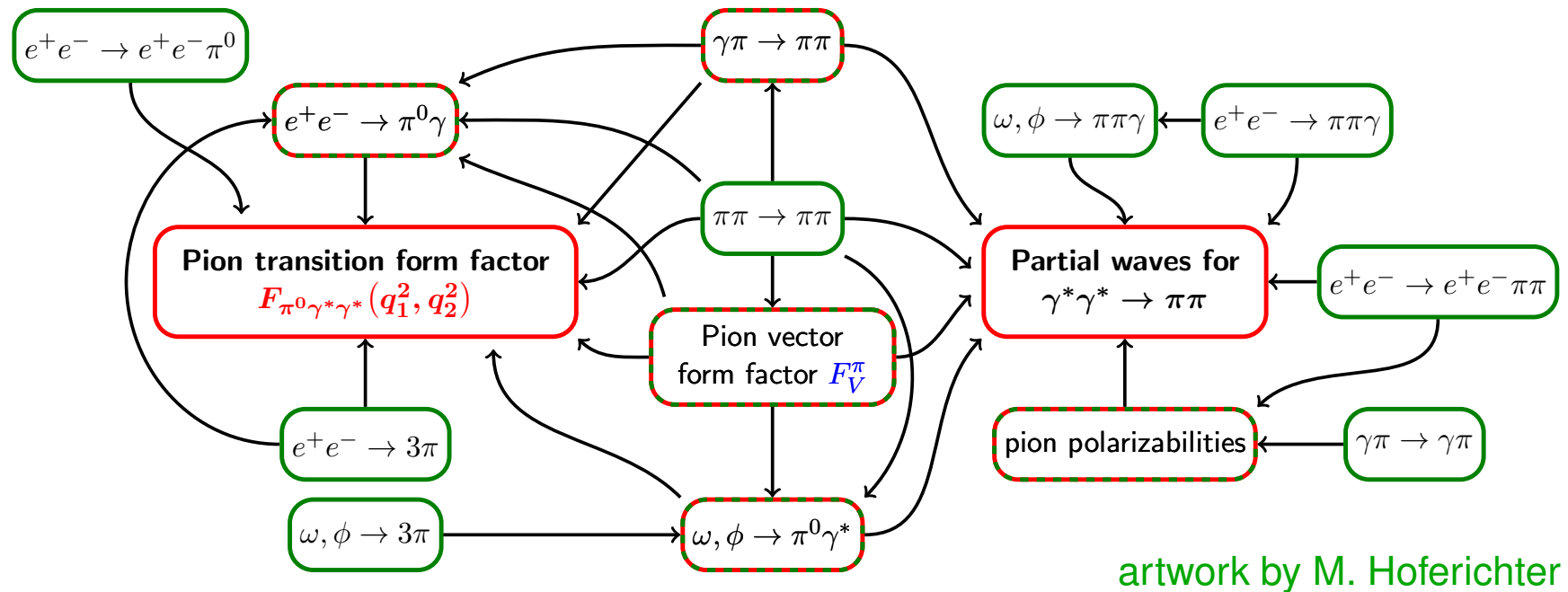
“White Paper” summary HLbL

hadronic state	$a_\mu^{\text{HLbL}} [10^{-11}]$	
pseudoscalar poles	$93.8^{+4.0}_{-3.6}$	η, η' : Masjuan, Sánchez-Puertas 2017
pion box	$-15.9(2)$	Colangelo et al. 2017
S-wave $\pi\pi$ rescatt.	$-8(1)$	Colangelo et al. 2017
kaon box	$-0.5(1)$	
scalars+tensors $\gtrsim 1$ GeV	$\sim -1(3)$	
axial vectors	$\sim 6(6)$	
short distance	$\sim 15(10)$	
heavy quarks	$\sim 3(1)$	
total	$92(19)$	Aoyama et al. 2020



→ further need for improvement to reach 10% accuracy for a_μ^{HLbL}

Summary: dispersion relations for HLbL



artwork by M. Hoferichter

Dispersive analyses of π^0 , $\eta^{(\prime)}$ transition form factors:

- QCD constraints + high-precision data on
 $e^+e^- \rightarrow \pi^+\pi^-(\pi^0)$ var. / $\eta \rightarrow \pi^+\pi^-\gamma$ KLOE / $\eta' \rightarrow \pi^+\pi^-\gamma$ BESIII
allow for high-precision dispersive predictions of π^0 , $\eta^{(\prime)} \rightarrow \gamma^*\gamma^{(*)}$

Main challenges for HLbL at 10% accuracy:

- matching low and high energies various

Spares

Form factors constrained by analyticity and unitarity

For illustration, let's briefly derive the Omnès solution!

- use $F_\pi^V(s) = P(s)\Omega(s)$: $\Omega(s)$ free of zeros, $\Omega(0) = 1$
- begin with the following simple manipulations:

$$\text{disc } \Omega(s) = 2i \Omega(s + i\epsilon) \times \sin \delta(s) e^{-i\delta(s)}$$

$$\Omega(s + i\epsilon) - \Omega(s - i\epsilon) = \Omega(s + i\epsilon) \times (1 - e^{-2i\delta(s)})$$

$$\Omega(s + i\epsilon) = \Omega(s - i\epsilon) \times e^{2i\delta(s)}$$

$$\text{disc } \log \Omega(s) = 2i \delta(s)$$

Form factors constrained by analyticity and unitarity

For illustration, let's briefly derive the Omnès solution!

- use $F_\pi^V(s) = P(s)\Omega(s)$: $\Omega(s)$ free of zeros, $\Omega(0) = 1$
- begin with the following simple manipulations:

$$\text{disc } \Omega(s) = 2i \Omega(s + i\epsilon) \times \sin \delta(s) e^{-i\delta(s)}$$

$$\Omega(s + i\epsilon) - \Omega(s - i\epsilon) = \Omega(s + i\epsilon) \times (1 - e^{-2i\delta(s)})$$

$$\Omega(s + i\epsilon) = \Omega(s - i\epsilon) \times e^{2i\delta(s)}$$

$$\text{disc } \log \Omega(s) = 2i \delta(s)$$

- this allows to write a dispersion relation for $\text{disc } \log \Omega(s)$:

$$\log \Omega(s) = \frac{s}{2\pi i} \int_{4M_\pi^2}^\infty ds' \frac{\text{disc } \log \Omega(s')}{s'(s' - s)} = \frac{s}{\pi} \int_{4M_\pi^2}^\infty ds' \frac{\delta(s')}{s'(s' - s)}$$

$$\Omega(s) = \exp \left\{ \frac{s}{\pi} \int_{4M_\pi^2}^\infty ds' \frac{\delta(s')}{s'(s' - s)} \right\}$$

Pion loop contributions / $\pi\pi$ intermediate states

Colangelo, Hoferichter, Procura, Stoffer 2017 [figs. courtesy of M. Hoferichter]

Decompose light-by-light scattering tensor $\Pi_{\mu\nu\lambda\sigma}$ into

- form factor scalar QED part \longrightarrow preserves gauge invariance

$$\Pi_{\mu\nu\lambda\sigma}^{\text{FsQED}} = F_\pi^V(q_1^2)F_\pi^V(q_2^2)F_\pi^V(q_3^2) \times \left[\begin{array}{c} \text{Three Feynman diagrams for } \pi\text{-box contribution} \\ \text{Diagram 1: Three vertices connected by dashed lines in a 2x2 grid.} \\ \text{Diagram 2: Three vertices connected by dashed lines in a 2x2 grid with a diagonal line.} \\ \text{Diagram 3: Three vertices connected by dashed lines in a 2x2 grid with a curved line.} \end{array} \right]$$

\longrightarrow $a_\mu^{\pi\text{-box}} = -15.9(2) \times 10^{-11}$

Pion loop contributions / $\pi\pi$ intermediate states

Colangelo, Hoferichter, Procura, Stoffer 2017 [figs. courtesy of M. Hoferichter]

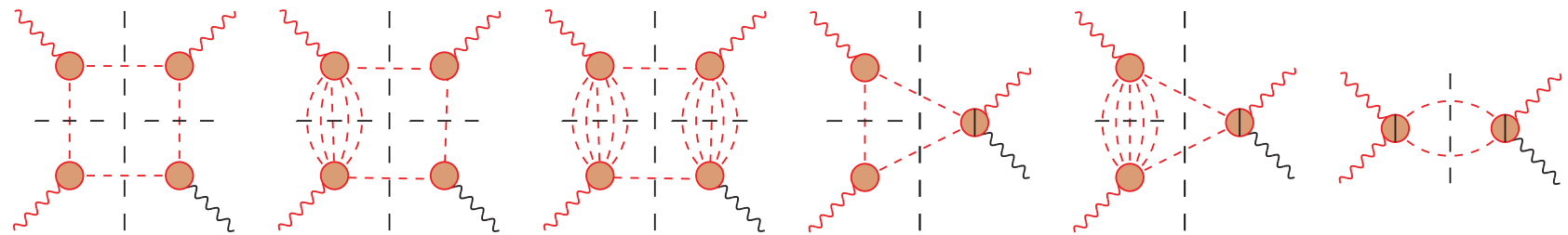
Decompose light-by-light scattering tensor $\Pi_{\mu\nu\lambda\sigma}$ into

- form factor scalar QED part \rightarrow preserves gauge invariance

$$\Pi_{\mu\nu\lambda\sigma}^{\text{FsQED}} = F_\pi^V(q_1^2)F_\pi^V(q_2^2)F_\pi^V(q_3^2) \times \left[\begin{array}{c} \text{Diagram 1} \\ \text{Diagram 2} \\ \text{Diagram 3} \end{array} \right]$$

$\rightarrow a_\mu^{\pi\text{-box}} = -15.9(2) \times 10^{-11}$

- + remainder $\bar{\Pi}_{\mu\nu\lambda\sigma}$ expanded in $\gamma^*\gamma^* \rightarrow \pi\pi$ helicity partial waves



organised according to left-hand-cut structure

S-wave rescattering $\rightarrow a_\mu^{\pi\pi, S\text{-wave}} = -8(1) \times 10^{-11}$

Pion loop contributions / $\pi\pi$ intermediate states

Colangelo, Hoferichter, Procura, Stoffer 2017 [figs. courtesy of M. Hoferichter]

Decompose light-by-light scattering tensor $\Pi_{\mu\nu\lambda\sigma}$ into

- form factor scalar QED part \rightarrow preserves gauge invariance

$$\Pi_{\mu\nu\lambda\sigma}^{\text{FsQED}} = F_\pi^V(q_1^2)F_\pi^V(q_2^2)F_\pi^V(q_3^2) \times \left[\begin{array}{c} \text{diagrams} \\ \text{(3 boxes)} \end{array} \right]$$

$\longrightarrow \boxed{a_\mu^{\pi\text{-box}} = -15.9(2) \times 10^{-11}}$

- + remainder $\bar{\Pi}_{\mu\nu\lambda\sigma}$ expanded in $\gamma^*\gamma^* \rightarrow \pi\pi$ helicity partial waves
- contains automatically
 - ▷ polarisability effects Engel, Patel, Ramsey-Musolf 2012
 - ▷ $\pi\pi$ resonances: $f_0(500)$ [$f_2(1270)$]
 - ▷ can be extended to $K\bar{K}$ ($\rightarrow f_0(980)$)

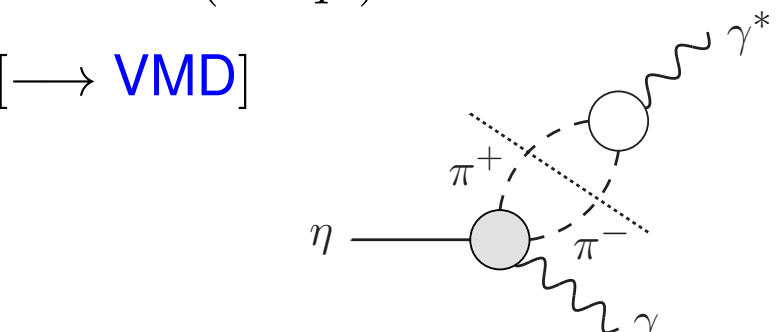
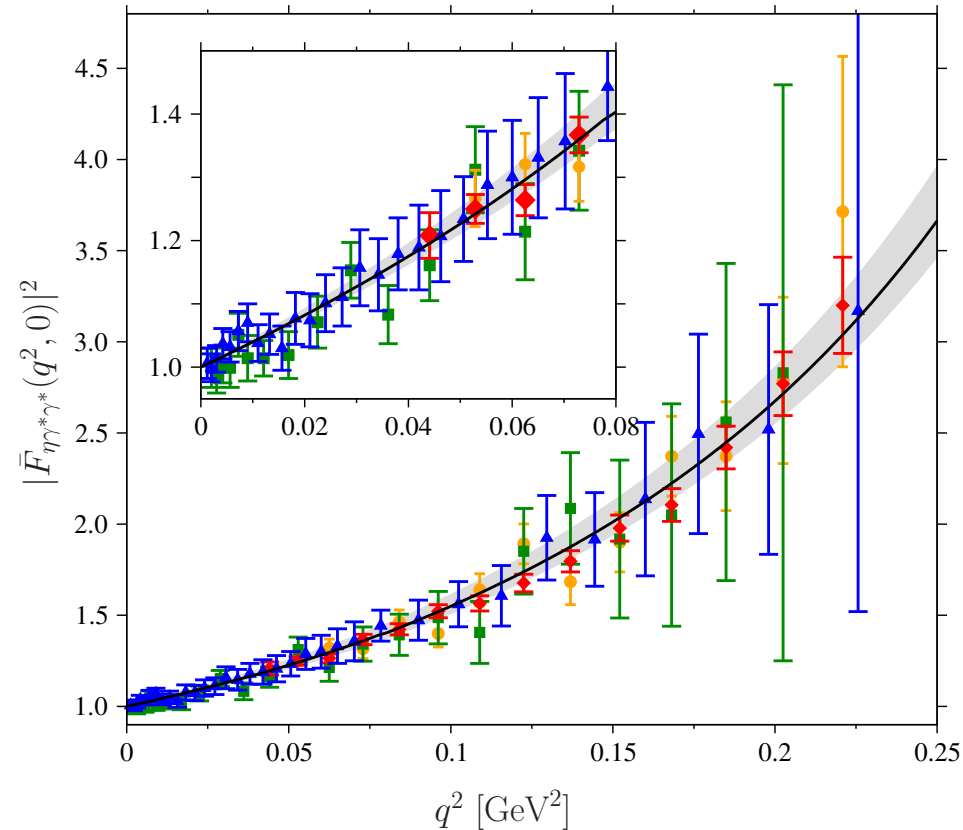
Danilkin, Deineka, Vanderhaeghen 2019; Danilkin, Hoferichter, Stoffer 2021

Transition form factor $\eta \rightarrow \gamma^* \gamma$

Hanhart et al. 2013, BK, Plenter 2015

$$F_{\eta\gamma^*\gamma}(q^2, 0) = F_{\eta\gamma\gamma} + \frac{q^2}{12\pi^2} \int_{4M_\pi^2}^\infty dt \frac{q_\pi^3(t) [F_\pi^V(t)]^* F_{\eta\pi\pi\gamma}(t)}{t^{3/2}(t - q^2)}$$

$$+ \Delta F_{\eta\gamma^*\gamma}^{I=0}(q^2, 0) \quad [\rightarrow \text{VMD}]$$



→ statistical advantage of
hadronic $\eta \rightarrow \pi^+ \pi^- \gamma$
 over direct $\eta \rightarrow \ell^+ \ell^- \gamma$
 (rate suppressed $\propto \alpha_{\text{QED}}^2$)

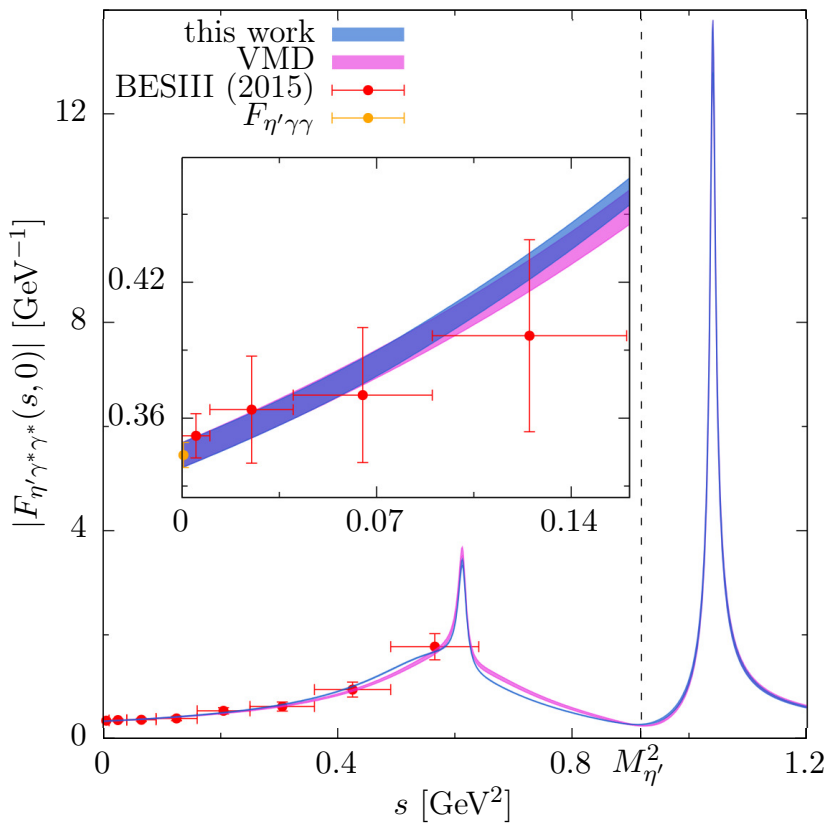
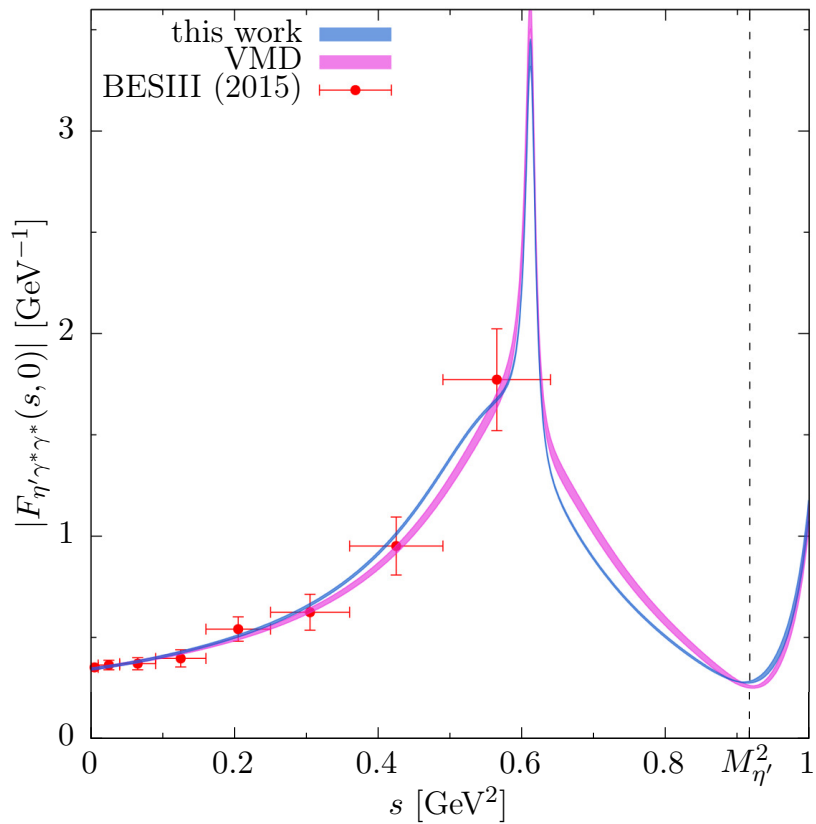
data: NA60 2009, 2016

A2 2014, 2017

Transition form factor $\eta' \rightarrow \gamma^* \gamma$

$$F_{\eta' \gamma^* \gamma}(q^2, 0) = F_{\eta' \gamma \gamma} + \frac{q^2}{12\pi^2} \int_{4M_\pi^2}^\infty dt \frac{q_\pi^3(t) [F_\pi^V(t)]^* F_{\eta' \pi \pi \gamma}(t)}{t^{3/2}(t - q^2)}$$

$$+ \Delta F_{\eta \gamma^* \gamma}^{I=0}(q^2, 0) \text{ [VMD]} + \text{[consistent isospin breaking]}$$



Holz, Hanhart, Hoferichter, BK 2022; data: BESIII 2015